Additional File 2

Complete figure of Support Clustering Analysis of normal and tumor SAGE libraries of the stomach. The figure provided represent normal libraries CGAP_MD_13S, GSM784, CGAP_MD_14S, GSM14780 (lines 1–4), West tumor libraries CGAP_MD_HG7, CGAP_MD_HS29, CGAP_MD_G329, GSM757, GSM758, GSM14760, GSM2385 (lines 5–11) and East tumor libraries GSM7800, GSM8505, and GSM8867 (lanes 12–14).
Click here for file
[http://www.biomedcentral.com/content/supplementary/1476-4598-7-22-S2.png]

Additional File 3

Complete figure of Support Clustering Analysis of West and East tumor SAGE libraries of the stomach. The figure provided represent West tumor libraries (CGAP_MD_HG7, CGAP_MD_HS29, CGAP_MD_G329, GSM757, GSM758, GSM14760, GSM2385) (lanes 1–7) and East tumor libraries (GSM7800, GSM8505, and GSM8867) (lanes 8–10).
Click here for file
[http://www.biomedcentral.com/content/supplementary/1476-4598-7-22-S3.png]

Additional File 4

Table S1. The significant tags with higher expression in Normal by Significant Analysis for Microarray between Normal and Tumor SAGE libraries. Only the tags that were successfully associated with a specific gene are shown. The tags are sorted in a significance descending order.
Click here for file
[http://www.biomedcentral.com/content/supplementary/1476-4598-7-22-S4.doc]

Additional File 5

Table S2. The significant tags with higher expression in Tumor by Significant Analysis for Microarray between Normal and Tumor SAGE libraries. Only the tags that were successfully associated with a specific gene are shown. The tags are sorted in a significance descending order.
Click here for file
[http://www.biomedcentral.com/content/supplementary/1476-4598-7-22-S5.doc]

Acknowledgements

We thank David S. Holmes and Gonzalo Riadi from Center for Bioinformatics and Genome Biology, Life Science Foundation – Andres Bello University, Santiago, Chile and Wael El-Rifai from Surgical Oncology Branch Vanderbilt Ingram Cancer Center, Vanderbilt University, Nashville, TN, USA, for helpful discussion of the manuscript. This work was supported by Chilean government research grants FONDECYT 1030130 and FONIS SA06I20019 to AHC.

References

1. Crew KD, Neugut AI: **Epidemiology of gastric cancer.** *World J Gastroenterol* 2006, **12**:354-362.
2. Pisani P, Bray F, Parkin DM: **Estimates of the world-wide prevalence of cancer for 25 sites in the adult population.** *Int J Cancer* 2002, **97**:72-81.
3. Parkin DM: **International variation.** *Oncogene* 2004, **23**:6329-6340.
4. Theuer CP, Kurosaki T, Ziogas A, Butler J, Anton-Culver H: **Asian patients with gastric carcinoma in the United States exhibit unique clinical features and superior overall and cancer specific survival rates.** *Cancer* 2000, **89**:1883-1892.
5. Theuer CP: **Ethnicity-related gastric cancer survival.** *J Clin Oncol* 2003, **21**:4253; author reply 4253.
6. Murray D, Doran P, MacMathuna P, Moss AC: **In silico gene expression analysis--an overview.** *Mol Cancer* 2007, **6**:50.
7. Riggins GJ, Strausberg RL: **Genome and genetic resources from the Cancer Genome Anatomy Project.** *Human Molecular Genetics* 2001, **10**:663-667.
8. El-Rifai W, Moskaluk CA, Abdrabbo MK, Harper J, Yoshida C, Riggins GJ, Frierson HF Jr., Powell SM: **Gastric cancers overexpress S100A calcium-binding proteins.** *Cancer Research* 2002, **62**:6823-6826.
9. Oue N, Hamai Y, Mitani Y, Matsumura S, Oshimo Y, Aung PP, Kuraoka K, Nakayama H, Yasui W: **Gene expression profile of gastric carcinoma: identification of genes and tags potentially involved in invasion, metastasis, and carcinogenesis by serial analysis of gene expression.** *Cancer Research* 2004, **64**:2397-2405.
10. Saeed AI, Sharov V, White J, Li J, Liang W, Bhagabati N, Braisted J, Klapa M, Currier T, Thiagarajan M, Sturn A, Snuffin M, Rezantsev A, Popov D, Ryltsov A, Kostukovich E, Borisovsky I, Liu Z, Vinsavich A, Trush V, Quackenbush J: **TM4: a free, open-source system for microarray data management and analysis.** *Biotechniques* 2003, **34**:374-378.
11. Boon K, Osorio EC, Greenhut SF, Schaefer CF, Shoemaker J, Polyak K, Morin PJ, Buetow KH, Strausberg RL, De Souza SJ, Riggins GJ: **An anatomy of normal and malignant gene expression.** *Proc Natl Acad Sci U S A* 2002, **99**:11287-11292.
12. Bala P, Georgantas RW 3rd, Sudhir D, Suresh M, Shanker K, Vrushabendra BM, Civin CI, Pandey A: **TAGmapper: a web-based tool for mapping SAGE tags.** *Gene* 2005, **364**:123-129.
13. Al-Shahrour F, Minguez P, Tarraga J, Montaner D, Alloza E, Vaquerizas JM, Conde L, Blaschke C, Vera J, Dopazo J: **BABELOMICS: a systems biology perspective in the functional annotation of genome-scale experiments.** *Nucleic Acids Research* 2006, **34**:W472-6.
14. Al-Shahrour F, Minguez P, Vaquerizas JM, Conde L, Dopazo J: **BABELOMICS: a suite of web tools for functional annotation and analysis of groups of genes in high-throughput experiments.** *Nucleic Acids Research* 2005, **33**:W460-4.
15. Feng B, Xu WB, Zheng MH, Ma JJ, Cai Q, Zhang Y, Ji J, Lu AG, Qu Y, Li JW, Wang ML, Hu WG, Liu BY, Zhu ZG: **Clinical significance of human kallikrein 10 gene expression in colorectal cancer and gastric cancer.** *J Gastroenterol Hepatol* 2006, **21(10)**:1596-1603.
16. Hanahan D, Weinberg RA: **The hallmarks of cancer.** *Cell* 2000, **100**:57-70.
17. Abelev GI, Lazarevich NL: **Control of differentiation in progression of epithelial tumors.** *Adv Cancer Res* 2006, **95**:61-113.
18. Luo A, Kong J, Hu G, Liew CC, Xiong M, Wang X, Ji J, Wang T, Zhi H, Wu M, Liu Z: **Discovery of Ca2+-relevant and differentiation-associated genes downregulated in esophageal squamous cell carcinoma using cDNA microarray.** *Oncogene* 2004, **23**:1291-1299.
19. Ben-Porath I, Kozak CA, Benvenisty N: **Chromosomal mapping of Tmp (Emp1), Xmp (Emp2), and Ymp (Emp3), genes encoding membrane proteins related to Pmp22.** *Genomics* 1998, **49**:443-447.

Publish with **BioMed Central** and every scientist can read your work free of charge

"BioMed Central will be the most significant development for disseminating the results of biomedical research in our lifetime."

Sir Paul Nurse, Cancer Research UK

Your research papers will be:

- available free of charge to the entire biomedical community
- peer reviewed and published immediately upon acceptance
- cited in PubMed and archived on PubMed Central
- yours — you keep the copyright

Submit your manuscript here:
http://www.biomedcentral.com/info/publishing_adv.asp

BioMedcentral

Reg IV is an independent prognostic factor for relapse in patients with clinically localized prostate cancer

Shinya Ohara,[1,2] Naohide Oue,[1] Akio Matsubara,[2] Koji Mita,[2] Yasuhisa Hasegawa,[2] Tetsutaro Hayashi,[2] Tsuguru Usui,[2] Vishwa Jeet Amatya,[3] Yukio Takeshima,[3] Hiroki Kuniyasu[4] and Wataru Yasui[1,5]

[1]Department of Molecular Pathology, [2]Department of Urology, and [3]Department of Pathology, Hiroshima University Graduate School of Biomedical Sciences, 1-2-3 Kasumi, Minami-ku, Hiroshima 734-8551; [4]Department of Molecular Pathology, Nara Medical University, 840 Shijo-cho, Kashihara, Nara 634-8521, Japan

(Received January 8, 2008/Revised April 10, 2008/Accepted April 10, 2008/Online publication July 29, 2008)

Regenerating islet-derived family, member 4 (*REG4*, which encodes Reg IV) is a candidate marker for cancer and inflammatory bowel disease. We investigated the potential prognostic role of Reg IV immunostaining in clinically localized prostate cancer (PCa) after radical prostatectomy. Immunohistochemical staining of Reg IV was performed in 98 clinically localized PCa tumors obtained during curative radical prostatectomy. Intestinal and neuroendocrine differentiation was investigated by MUC2 and chromogranin A immunostaining, respectively. The prognostic significance of immunohistochemical staining for these factors on prostate-specific antigen (PSA)-associated recurrence was assessed by Kaplan–Meier analysis and a Cox regression model. Phosphorylation of the epidermal growth factor receptor (EGFR) by Reg IV was analyzed by Western blot. In total, 14 (14%) of the 98 PCa cases were positive for Reg IV staining. Reg IV positivity was observed frequently in association with MUC2 ($P = 0.0182$) and chromogranin A positivity ($P = 0.0012$). Univariate analysis revealed that Reg IV staining ($P = 0.0004$), chromogranin A staining ($P = 0.0494$), Gleason score ($P < 0.0001$) and preoperative PSA concentration ($P = 0.0167$) were significant prognostic factors for relapse-free survival. Multivariate analysis indicated that Reg IV staining ($P = 0.0312$), Gleason score ($P = 0.0014$) and preoperative PSA concentration ($P = 0.0357$) were independent predictors of relapse-free survival. In the LNCaP cell line, EGFR phosphorylation was induced by the addition of Reg IV-conditioned medium. These results suggest that Reg IV expression is an independent prognostic indicator of relapse after radical prostatectomy. (*Cancer Sci* 2008; 99: 1570–1577)

Prostate cancer (PCa) is one of the most common cancers and the second leading cause of cancer death in men in the USA.[1] PCa screening by assessing serum prostate-specific antigen (PSA) level has led to increased detection of early stage PCa that can be cured by radical prostatectomy or radiation therapy. Nonetheless, a substantial fraction of patients with clinically localized PCa who undergo curative radical prostatectomy will eventually recur with metastatic disease. These patients would benefit most from the discovery of a prognostic factor that can identify individuals for whom adjuvant therapy would be advantageous. Treatment decisions are based mainly on known prognostic factors. High risk of relapse is defined according to preoperative PSA level (>20 ng/mL), biopsy Gleason score (≥8), and the 1992 American Joint Committee on Cancer (AJCC) clinical T stage (≥T2c).[2] These factors are helpful but far from perfect due to significant clinical heterogeneity. Clearly, new biological markers are needed to accurately predict the risk of relapse.

We previously performed serial analysis of gene expression of four primary gastric cancers,[3] and identified several gastric cancer-specific genes.[4] Of these genes, regenerating islet-derived family, member 4 (*REG4*, which encodes Reg IV) is a candidate gene for cancer-specific expression, at least in patients with gastric cancer. Although various normal tissues express *REG4*, the levels of expression are much lower in normal tissues than in cancerous tissues.[3] Our previous immunohistochemical analysis revealed that Reg IV was expressed in 30% of gastric cancers and was associated with both intestinal mucin phenotype and neuroendocrine differentiation.[5] Reg IV is a secreted protein, and we also showed that serum Reg IV represents a novel biomarker for gastric cancer.[6]

Understanding of the genetic and epigenetic pathways involved in the pathogenesis of PCa is essential for the development of improved diagnostic and treatment modalities. A variety of genetic and epigenetic alterations is associated with PCa.[7,8] In addition to gastric, colorectal,[9] and pancreatic[10] cancers, overexpression of *REG4* mRNA in PCa has been reported by *in situ* hybridization.[11] The majority of localized PCa tumors expressed a low level of *REG4* mRNA, whereas the majority of metastatic PCa tumors expressed a high level of *REG4* mRNA. Although the biological function of Reg IV is poorly understood, it has been reported that Reg IV is a potent activator of the epidermal growth factor receptor (EGFR)/Akt/activator protein-1 (AP-1) signaling pathway in colon cancer cells and increases expression of Bcl-2, Bcl-xl and surviving, proteins associated with the inhibition of apoptosis.[12] We have also reported that forced expression of Reg IV induces phosphorylation of the EGFR and inhibits 5-fluorouracil-induced apoptosis in gastric cancer cells.[6] Taken together, these findings suggest that Reg IV may also participate in tumor cell growth in PCa and may be a new prognostic marker for relapse in patients with PCa. However, the expression and distribution of Reg IV protein and the biological significance of Reg IV in PCa has not been investigated.

In the present retrospective study, we examined the expression and distribution of Reg IV in 98 clinically localized PCa tumors by immunohistochemistry. The relation between staining for Reg IV and clinicopathological characteristics was also examined. We have reported two Reg IV staining patterns (mucin-like staining and perinuclear staining).[5] Mucin-like staining, observed in goblet cells and goblet cell-like vesicles of tumor cells, is associated with MUC2 (a marker of goblet cells) positivity. Perinuclear staining is detected in cells with neuroendocrine differentiation and that show chromogranin A (a marker of neuroendocrine cells) positivity. Therefore, we examined staining for Reg IV and chromogranin A or MUC2 by double-immunofluorescence. Because Reg IV activates the EGFR, we also performed an immunohistochemical analysis of Reg IV and EGFR expression.

[5]To whom correspondence should be addressed. E-mail: wyasui@hiroshima-u.ac.jp

doi: 10.1111/j.1349-7006.2008.00846.x
© 2008 Japanese Cancer Association

Materials and Methods

Tissue samples. Ninety-eight primary tumors were collected from patients diagnosed with PCa who underwent surgery during 2000–2002 at the Department of Urology, Hiroshima University Hospital (Hiroshima, Japan). All 98 patients were treated by radical prostatectomy and bilateral lymphadenectomy for clinically localized PCa and were confirmed to be node negative by pathological examination. None of the patients were treated preoperatively with hormonal or radiation therapy, and none had secondary cancer. All 98 specimens were archival, formalin-fixed, paraffin-embedded tissues. Tumor staging was performed according to the AJCC classification system. After prostatectomy, the serum PSA level was measured by *E*-test Tosoh II Assay (Tosoh, Tokyo, Japan). Patients were followed up by PSA measurement monthly during the first 6 months after prostatectomy and then every 3 months thereafter. Biochemical relapse was defined as a PSA level of 0.2 ng/mL or greater. Because written informed consent was not obtained, for strict privacy protection, identifying information for all samples was removed before analysis. This procedure was in accordance with the Ethical Guidelines for Human Genome/Gene Research of the Japanese Government.

Immunohistochemistry. Formalin-fixed, paraffin-embedded samples were sectioned, deparaffinized and stained with hematoxylin–eosin to ensure that the sectioned block contained tumor cells. Adjacent sections were then stained immunohistochemically. Antigen retrieval was performed by microwave heating in citrate buffer (pH 6.0) for 30 min for Reg IV, MUC2, chromogranin A, EGFR, phospho-EGFR (Tyr^{1068}) and transforming growth factor (TGF)-α. Peroxidase activity was blocked with 3% H_2O_2-methanol for 10 min, and sections were then incubated with normal goat serum (Dako Cytomation, Carpinteria, CA, USA) for 20 min to block nonspecific antibody binding. Sections were incubated with primary antibody against Reg IV (rabbit polyclonal antibody, diluted 1:50; anti-Reg IV antibody was raised in our laboratory),[5] MUC2 (1:50; Novocastra, Newcastle, UK), chromogranin A (1:50; Novocastra), EGFR (1:50; Dako Cytomation), phospho-EGFR (Tyr^{1068}) (1:50; Cell Signaling Technology, Beverly, MA, USA) or TGF-α (Calbiochem, San Diego, CA, USA) for 1 h at room temperature, followed by incubation with peroxidase-labeled antirabbit or antimouse IgG for 1 h. Staining was completed with a 10-min incubation in substrate–chromogen solution. The sections were counterstained with 0.1% hematoxylin. The specificity of the Reg IV antibody has been characterized in detail elsewhere.[5]

Double-immunofluorescence staining was performed as described previously.[5] Alexa Fluor 546-conjugated antirabbit immunoglobulin (Ig)G (Molecular Probes, Eugene, OR, USA) and Alexa Fluor 488-conjugated antimouse IgG (Molecular Probes) were used as secondary antibodies.

The specificity of immunohistochemical detection for Reg IV was verified by triple-immunofluorescence staining with different antibodies against Reg IV (goat polyclonal, rabbit polyclonal and mouse monoclonal). Goat polyclonal and mouse monoclonal anti-Reg IV antibodies were purchased from R&D Systems (Abingdon, UK). Alexa Fluor 405-conjugated antigoat IgG (Molecular Probes), Alexa Fluor 488-conjugated antimouse IgG (Molecular Probes) and Alexa Fluor 546-conjugated antirabbit IgG (Molecular Probes) were used as secondary antibodies.

Cell culture and conditioned medium production. Colon cancer cell line, colo320, and human prostate cell line, LNCaP, were maintained in RPMI-1640 medium (Nissui Pharmaceutical, Tokyo, Japan) containing 10% fetal bovine serum (FBS) (Whittaker, Walkersville, MD, USA) at 37°C in a humidified atmosphere of 5% CO_2 and 95% air. Reg IV-conditioned medium (Reg IV-CM) and colo320 control medium were prepared as follows. Colo320 cells stably transfected with a Reg IV cDNA were grown to 80–90% confluence in RPMI-1640 medium containing 10% FBS. The medium was removed and the cells were washed twice with phosphate-buffered saline (PBS). Cells were incubated for 48 h in 20 mL serum-free RPMI-1640 medium. After 48 h, the medium was collected and filtered (0.22-μm pores; Becton Dickinson Labware, Bedford, MA, USA). Control medium from colo320 cells stably transfected with the pcDNA3.1 vector alone was prepared under the same conditions. Conditioned medium was then normalized for DNA content between samples by adding RPMI-1640 medium. Levels of EGF and TGF-α in Reg IV-CM and control medium were assessed by sandwich-type enzyme-linked immunosorbent assay (ELISA) (R&D Systems).

Western blot analysis. Western blot analysis was performed as described previously.[13] To examine whether Reg IV activates phosphorylation of the EGFR, cells were serum starved for 24 h and treated with Reg IV-CM or control medium for 3 min. To examine whether EGF or TGF-α induce Reg IV expression, cells were serum starved for 24 h and treated with EGF (100 nM, Sigma, Saint Louis, MO, USA) or TGF-α (10 nM, Sigma) for 1, 2 and 3 days. Cells were scraped in PBS supplemented with 1 mM Na_3VO_4, centrifuged, and lysed in ice-cold RIPA buffer (20 mM Tris-HCl [pH 7.5], 0.15 M NaCl, 1% Triton X-100, 1 mM phenylmethylsulfonyl fluoride, 1 mM Na_3VO_4, 1 mM ethyleneglycotetraacetic acid [EGTA], 1 μg/mL leupeptin, 2 μg/mL aprotinin and 10 μg/mL pepstatin). Supernatant protein concentration was measured with a the Bio-Rad Protein Assay kit (Bio-Rad, Hercules, CA, USA). Protein (20 μg/lane) was electrophoresed on sodium dodecylsulfate polyacrylamide gel electrophoresis (SDS-PAGE) gels and transferred to nitrocellulose filters. Filters were incubated for 1 h at room temperature with anti-Reg IV antibody (rabbit polyclonal antibody raised in our laboratory),[5] anti-EGFR antibody (Cell Signaling Technology), antiphospho-EGFR (Tyr^{992}) antibody (Cell Signaling Technology) or antiphospho-EGFR (Tyr^{1068}) antibody (Cell Signaling Technology).

Statistical methods. Association between clinicopathological variables and Reg IV expression was analyzed by Fisher's exact test. Kaplan–Meier survival curves were constructed for Reg IV-positive and Reg IV-negative patients. Survival rates were compared between Reg IV-positive and Reg IV-negative groups. Differences in survival between groups were tested for statistical significance by log–rank test.[14] The Cox proportional hazards multivariate model was used to examine the association of clinical and pathological factors and Reg IV and chromogranin A staining with survival. $P < 0.05$ was considered statistically significant.

Results

Immunohistochemical analysis of Reg IV in PCa tissues. We performed an immunohistochemical analysis of Reg IV expression in 98 clinically localized PCa cases. In adjacent non-neoplastic prostate tissue, focal Reg IV staining was found in five (5%) of 98 cases. Periodic luminal epithelial cells stained for Reg IV, but stromal cells showed no staining for Reg IV (Fig. 1a). We confirmed that Reg IV-positive cells were not stained by 34βE12 (a marker of basal cells) (Fig. 1b). Although the specificity of the Reg IV antibody has been characterized in detail,[5] the specificity of immunohistochemical detection for Reg IV was further verified by triple-immunofluorescence staining with different antibodies against Reg IV (goat polyclonal, rabbit polyclonal and mouse monoclonal). Cells stained with anti-Reg IV goat polyclonal antibody also stained with anti-Reg IV rabbit polyclonal antibody and anti-Reg IV mouse monoclonal antibody, indicating that these anti-Reg IV antibodies specifically

© 2008 Japanese Cancer Association

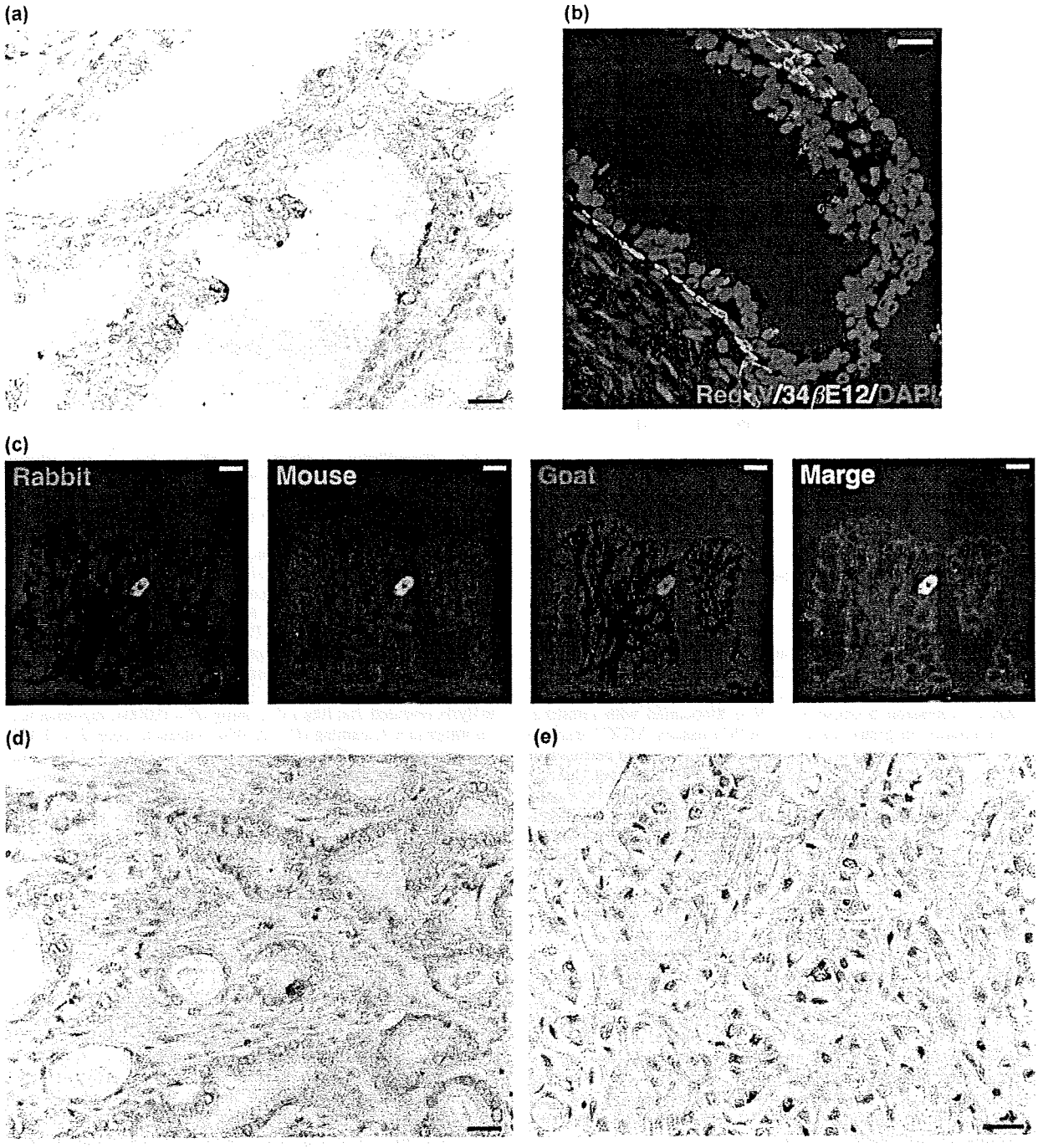

Fig. 1. Immunohistochemical analysis of Reg IV expression in clinically localized prostate cancer. (a) Immunostaining of Reg IV in adjacent non-neoplastic prostate tissue. Several luminal epithelial cells show Reg IV staining. Scale line, 25 μm. (b) Double-immunostaining of Reg IV (red) and 34βE12 (a marker for basal cells; green). Nuclei are stained with 4′,6-diamidino-2-phenylindole (DAPI; blue). Scale line, 25 μm. (c) Triple-immunostaining of rabbit polyclonal anti-Reg IV (red), mouse monoclonal anti-Reg IV (green), and goat polyclonal anti-Reg IV (blue). Scale line, 13 μm. (d) Immunostaining of Reg IV in prostate cancer (PCa). Mucin-like staining of Reg IV is present in goblet cell-like vesicles of tumor cells. Scale line, 25 μm. (e) Immunostaining of Reg IV in PCa. Perinuclear staining of Reg IV is present in tumor cells. Scale line, 25 μm.

recognize Reg IV protein (Fig. 1c). In PCa tissues, Reg IV staining was observed in 14 (14%) of 98 PCa cases. In all 14 PCa cases, few tumor cells (1–10%) showed Reg IV staining. Stromal cells showed no Reg IV staining. Reg IV staining was considered positive if any tumor cells were stained. In each Reg IV-positive case, both mucin-like staining (Fig. 1d) and perinuclear staining (Fig. 1e) were observed. We analyzed relations between Reg IV staining and clinicopathological

doi: 10.1111/j.1349-7006.2008.00846.x
© 2008 Japanese Cancer Association

Table 1. Association between Reg IV immunostaining and clinicopathological variables

	Reg IV		
	Positive	Negative	*P*-value
pT stage			
≤2b	6 (22%)	21	0.2001
≥2c	8 (11%)	63	
Gleason score			
≤7	8 (11%)	66	0.1001
≥8	6 (25%)	18	
Preoperative PSA concentration			
<20	12 (13%)	77	0.6122
≥20	2 (22%)	7	
MUC2			
Positive	14 (19%)	58	0.0182
Negative	0 (0%)	26	
Chromogranin A			
Positive	10 (32%)	21	0.0012
Negative	4 (6%)	63	
EGFR			
Positive	8 (32%)	17	0.0067
Negative	6 (8%)	67	
Phospho-EGFR (Tyr^{1068}) ($n = 25$)			
Positive	6 (67%)	3	0.0099
Negative	2 (13%)	14	

EGFR, epidermal growth factor receptor; PSA, prostate-specific antigen.

Table 2. Multivariate analysis of factors influencing relapse-free survival

	Hazard ratio	(95% CI)	χ^2-test	*P*-value
Reg IV staining				
Negative	1	(Reference)	4.640	0.0312
Positive	2.848	(1.099–7.381)		
Chromogranin A staining				
Negative	1	(Reference)	0.005	0.9431
Positive	1.034	(0.414–2.582)		
Gleason score				
≤7	1	(Reference)	10.235	0.0014
≥8	3.747	(1.668–8.416)		
Preoperative PSA concentration				
<20	1	(Reference)	4.410	0.0357
≥20	2.938	(1.074–8.036)		

CI, confidence interval; PSA, prostate-specific antigen.

characteristics. Reg IV staining was not correlated with pT stage, Gleason score or preoperative PSA concentration (Table 1).

We also performed an immunohistochemical analysis of MUC2 expression because Reg IV is associated with intestinal differentiation in gastric cancer.[5] In PCa tissues, MUC2 staining was observed in goblet cell-like vesicles (Fig. 2a) and perinuclear regions (Fig. 2b) of tumor cells. Of the 98 PCa cases, MUC2 staining was observed in 72 (73%). MUC2-positive PCa cells comprised 1–30% of tumor cells. MUC2 staining was considered positive if any tumor cells were stained. We analyzed the relation between MUC2 staining and clinicopathological characteristics. MUC2 positivity was found more frequently in PCa showing a pT stage of 2c or more (59/71, 83%) than in PCa showing a pT stage of 2b or less (13/27, 48%, $P = 0.0182$, Fisher's exact test). MUC2 staining was not correlated with Gleason score or preoperative PSA concentration. Association between Reg IV and MUC2 staining was also analyzed. Reg IV positivity was found more frequently in MUC2-positive cases (14/72, 19%) than in MUC2-negative cases (0/26, 0%, $P = 0.0182$, Fisher's exact test) (Table 1). We confirmed that almost all tumor cells showing mucin-like staining of Reg IV were positive for MUC2 by double-immunofluorescence staining (Fig. 2c). Some PCa cells showing perinuclear Reg IV staining also showed MUC2 staining (Fig. 2d). These results indicated that Reg IV is associated with intestinal differentiation of PCa.

Immunostaining of chromogranin A was also performed. Representative results of chromogranin A immunostaining in PCa are shown in Fig. 2(e). Of the 98 PCa cases, chromogranin A staining was observed in 31 (32%). Chromogranin A positivity was observed in 1–40% of PCa cells. Chromogranin A staining was considered positive if any tumor cells were stained. We analyzed the relation between chromogranin A staining and clinicopathological characteristics. Chromogranin A positivity were found more frequently in PCa showing a Gleason score of 8 or more (12/24, 50%) than in PCa showing a Gleason score of 7 or less (19/74, 26%, $P = 0.0418$, Fisher's exact test). Chromogranin A staining was not correlated with pT stage or preoperative PSA concentration. Association between Reg IV and chromogranin A staining was also analyzed. Reg IV positivity was found more frequently in chromogranin A-positive cases (10/31, 32%) than in chromogranin A-negative cases (4/67, 6%, $P = 0.0012$, Fisher's exact test) (Table 1). These results indicated that Reg IV is associated with neuroendocrine differentiation. However, double-immunofluorescence staining revealed that Reg IV-positive cells did not show chromogranin A staining (Fig. 2f). Therefore, a paracrine effect of secreted Reg IV may be involved in neuroendocrine differentiation in PCa.

Relation between Reg IV immunostaining and relapse-free survival of PCa patients. We next examined the relation between Reg IV immunostaining and relapse-free survival in PCa. Univariate analysis revealed that Reg IV staining ($P = 0.0004$, log–rank test), chromogranin A staining ($P = 0.0494$), Gleason score ($P < 0.0001$) and preoperative PSA concentration ($P = 0.0167$) (Fig. 3a–d) were significant prognostic factors for relapse-free survival in patients with PCa, whereas MUC2 staining and pT stage did not correlate with relapse-free survival. We then used the Cox proportional hazards multivariate model to examine the association of clinicopathological factors and Reg IV and chromogranin A staining with relapse-free survival. Multivariate analysis indicated that Reg IV staining, Gleason score and preoperative PSA concentration were independent predictors of relapse-free survival in patients with PCa (Table 2). These results suggested that Reg IV expression directly contributes to the malignant potential of PCa.

Reg IV activates EGFR in LNCaP cells. Statistical analysis revealed that Reg IV is an independent predictor of relapse-free survival in patients with clinically localized PCa. However, the underlying mechanism remains unclear. Therefore, Reg IV-CM was prepared and the function of Reg IV was analyzed. It has been reported that recombinant human Reg IV induces rapid phosphorylation of the EGFR at Tyr^{992} and Tyr^{1068} and of Akt at Thr^{308} and Ser^{473} resulting in increased AP-1 transcription factor activity.[12] Western blot analysis of the EGFR showed that colo320 did not express EGFR protein (data not shown). Therefore, we assumed that Reg IV overexpression has little effect in colo320 cells. Thus, Reg IV-CM was prepared with the colo320 cell line. With a specific antibody, we verified the expression of Reg IV protein in Reg IV-CM prepared from colo320 cells (Fig. 4a). We also examined whether EGF and TGF-α could be detected by ELISA in Reg IV-CM and control medium. EGF or TGF-α was not detected in Reg IV-CM or control medium (data not shown). We tested the specificity of the antiphospho-EGFR (Tyr^{1068}) and antiphospho-EGFR (Tyr^{992})

© 2008 Japanese Cancer Association

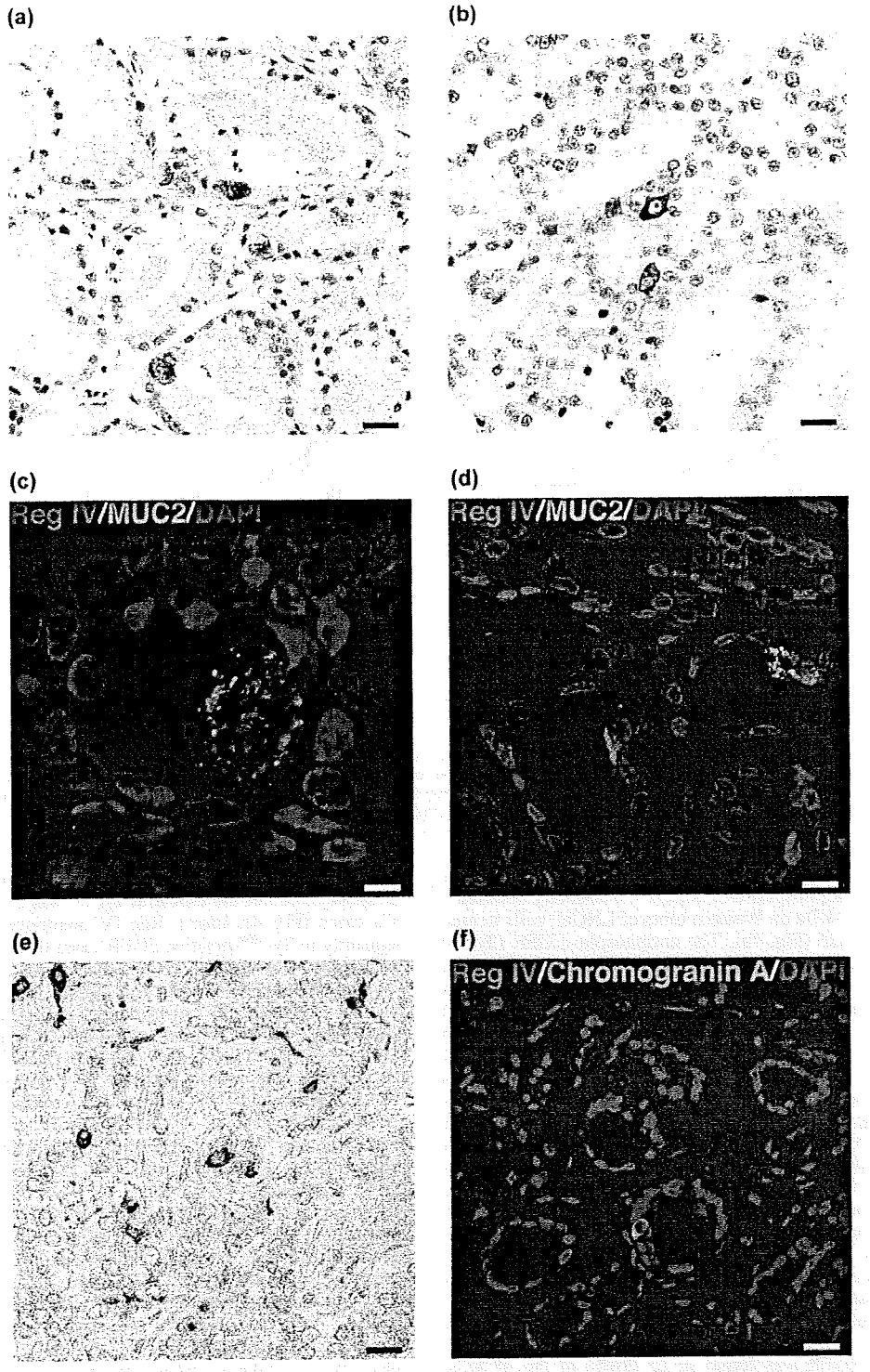

Fig. 2. Immunohistochemical analysis of MUC2 and chromogranin A expression in clinically localized prostate cancer (PCa). (a) Immunostaining of MUC2 in PCa. Mucin-like staining of MUC2 is present in goblet cell-like vesicles of a tumor cell. Scale line, 25 μm. (b) Immunostaining of MUC2 in PCa. Perinuclear staining of MUC2 is present in a tumor cell. Scale line, 25 μm. (c) Double-immunostaining of Reg IV (red) and MUC2 (green). Nuclei are stained with 4′,6-diamidino-2-phenylindole (DAPI; blue). Reg IV staining is present with MUC2 in goblet cell-like vesicles of a tumor cell. Scale line, 13 μm. (d) Double-immunostaining of Reg IV (red) and MUC2 (green). Nuclei are stained with DAPI (blue). A tumor cell showing perinuclear staining of Reg IV also shows MUC2 staining. Scale line, 25 μm. (e) Immunostaining of chromogranin A in PCa. Scale line, 25 μm. (f) Double-immunostaining of Reg IV (red) and chromogranin A (green). Nuclei are stained with DAPI (blue). Scale line, 25 μm.

doi: 10.1111/j.1349-7006.2008.00846.x
© 2008 Japanese Cancer Association

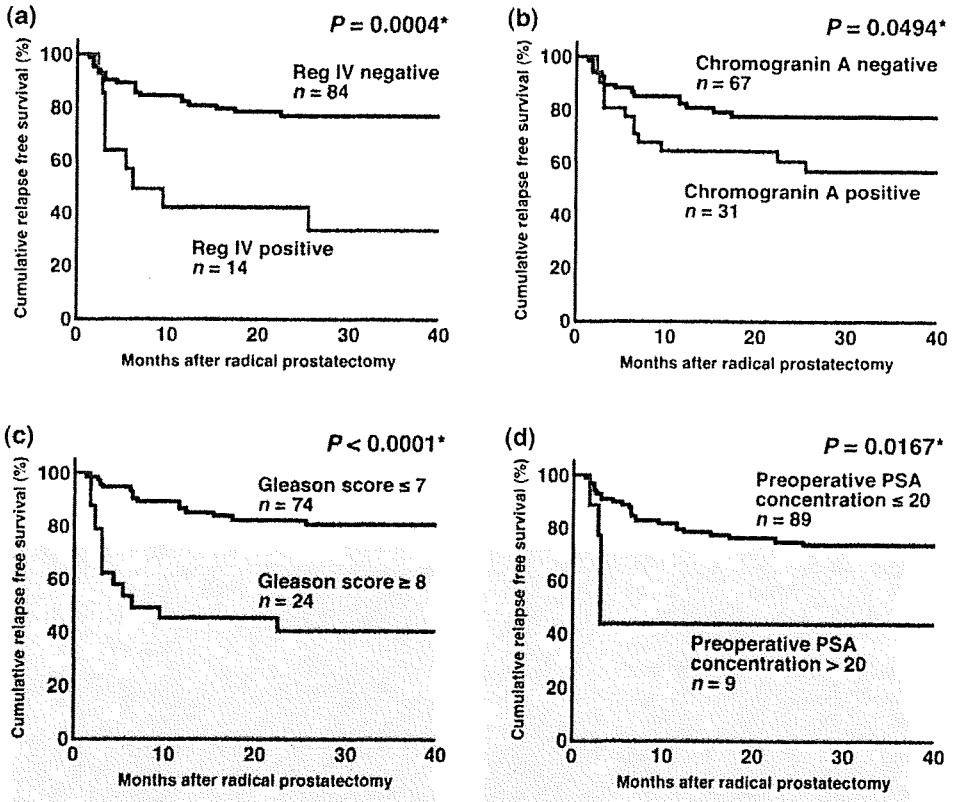

Fig. 3. Relapse-free survival of patients with prostate cancer (PCa). (a) Kaplan–Meier curves of patients with Reg IV-negative or Reg IV-positive PCa. (b) Kaplan–Meier curves of patients with chromogranin A-negative or chromogranin A-positive PCa. (c) Kaplan–Meier curves of patients with low Gleason score (≤7) or high Gleason score (≥8) PCa. (d) Kaplan–Meier curves of patients with low preoperative prostate specific antigen (PSA) concentration (≤20) or high preoperative PSA concentration (>20) PCa. *Log–rank test.

antibodies. Western blotting of lysates of LNCaP cell line was performed. The antiphospho-EGFR (Tyr^{1068}) antibody detected a single band of 170 kDa on Western blots of LNCaP cells treated with TGF-α or EGF (Fig. 4b). The antiphospho-EGFR (Tyr^{992}) antibody also detected a single band of 170 kDa on Western blots of LNCaP cells treated with TGF-α or EGF (data not shown). These data show that these antiphospho-EGFR (Tyr^{1068}) and antiphospho-EGFR (Tyr^{992}) antibodies specifically recognize phospho-EGFR protein. The effect of Reg IV-CM on EGFR phosphorylation was then investigated in LNCaP cells. EGFR was phosphorylated at Tyr^{1068} but not Tyr^{992} in LNCaP cells treated with Reg IV-CM (Fig. 4c). These findings indicated that Reg IV is involved in EGFR phosphorylation in an EGF- and TGF-α-independent manner in LNCaP cells. Because it has been reported that growth factors enhance *REG4* mRNA expression in colon cancer cells,[15] the effect of EGF and TGF-α on *REG4* expression was also investigated in LNCaP cells. Neither EGF or TGF-α had any significant effect on Reg IV protein expression in LNCaP cells (Fig. 4d). Similar results were also obtained from the DU145 cell line (data not shown).

We next examined whether expression of Reg IV activates phosphorylation of the EGFR at Tyr^{1068} in PCa tissue samples. Staining of the EGFR was found in 25 (26%) of the 98 PCa cases. All 25 PCa cases were considered EGFR-positive. Of 25 PCa cases positive for EGFR, eight (32%) were positive for Reg IV. In eight PCa cases positive for both Reg IV and EGFR, Reg IV-positive tumor cells were found near EGFR-positive tumor cells (Fig. 4e). Because Reg IV-CM phosphorylated the EGFR at Tyr^{1068} in LNCaP cells, we further investigated phosphorylation of the EGFR at Tyr^{1068} in 25 PCa cases positive for EGFR staining. Phosphorylation of the EGFR at Tyr^{1068} was found in nine (36%) PCa cases (Fig. 4e, inset). Reg IV positivity was found more frequently in Tyr^{1068}-positive EGFR cases than in Tyr^{1068}-negative EGFR cases ($P = 0.0099$, Fisher's exact test) (Table 1). Because it is possible that EGFR phosphorylation is due to the stimulation by some growth factors rather than Reg IV protein in the human PCa tissues, we performed immunohistochemical analysis of TGF-α. As reported previously,[16] in most cases, TGF-α expression was present in the stroma; however, co-expression of EGFR and TGF-α in tumor cells was observed in several PCa cases. Tumor cell staining of the TGF-α was found in 17 (17%) of the 98 PCa cases (Fig. 4f). We regarded these cases with TGF-α-positive tumor cells as TGF-α-positive. Of 25 PCa cases positive for EGFR, nine (36%) were positive for TGF-α. TGF-α positivity was found more frequently in Tyr^{1068}-positive EGFR cases (7/9, 78%) than in Tyr^{1068}-negative EGFR cases (2/16, 13%, $P = 0.0022$, Fisher's exact test). Because it has been reported that growth factors enhance *REG4* mRNA expression in colon cancer cells,[15] association between Reg IV and TGF-α staining was analyzed. Reg IV positivity was found more frequently in TGF-α-positive cases (8/17, 47%) than in TGF-α-negative cases (6/81, 7%, $P = 0.0003$, Fisher's exact test).

Discussion

Overexpression of *REG4* mRNA has been reported in PCa by *in situ* hybridization.[11] A majority of metastatic PCa tumors express high levels of *REG4* mRNA. In addition, *REG4*

© 2008 Japanese Cancer Association

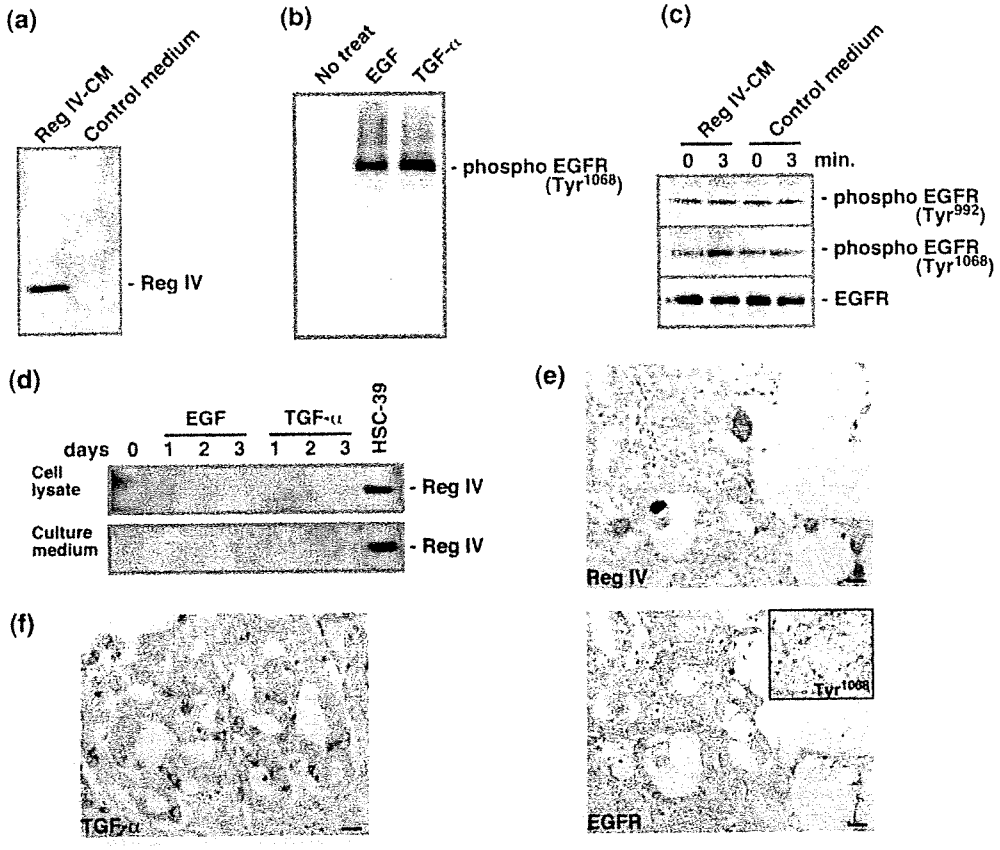

Fig. 4. Effect of Reg IV on epidermal growth factor receptor (EGFR) phosphorylation. (a) 10 μL of Reg IV-conditioned medium and control medium were analyzed by Western blot with a rabbit polyclonal antibody against Reg IV. (b) LNCaP cells were cultured with either EGF (100 nM) or transforming growth factor (TGF)-α (10 nM) for 3 min. Whole-cell lysates were prepared and analyzed by Western blot with antiphospho-EGFR (Tyr^{1068}) antibody. (c) LNCaP cells were cultured with either Reg IV-CM or control medium for 3 min. Whole-cell lysates were prepared and analyzed by Western blot with antiphospho-EGFR (Tyr^{992}) or antiphospho-EGFR (Tyr^{1068}) antibody. The samples were also probed with anti-EGFR antibody to verify equal loading. (d) LNCaP cells were cultured with either EGF (100 nM) or TGF-α (10 nM) for 1, 2 or 3 days. Whole-cell lysates and culture medium were analyzed by Western blot with anti-Reg IV antibody. (e) Expression of Reg IV and EGFR was examined by immunohistochemistry in serial sections of prostate cancer. Inset, phospho-EGFR (Tyr^{1068}) staining of a serial section. Scale line, 25 μm. (f) Expression of TGF-α was examined by immunohistochemistry. Scale line, 25 μm.

expression is significantly more intense in high-grade PCa (Gleason score, 7–10) than in low-grade PCa (Gleason score, 5–6). In the present study of clinically localized PCa, Reg IV-positive cases showed unfavorable prognosis with respect to relapse-free survival. Several autocrine and paracrine signaling pathways involving the EGFR and its ligands, EGF and TGF-α, are postulated to stimulate tumor cell proliferation independent of androgen activity.[17] These pathways become much more essential to PCa growth once androgen insensitivity occurs. EGFR signaling pathways are also involved in PCa invasion and angiogenesis, both of which are crucial for progression and metastasis.[18,19] In the present study, we showed that Reg IV-CM phosphorylated the EGFR at Tyr^{1068}. These findings suggest that Reg IV activates phosphorylation of the EGFR in human PCa tissues. Although the precise mechanism of EGFR phosphorylation by Reg IV remains unclear, it is not likely that secretion of the EGFR ligands, such as EGF and TGF-α, is involved because no EGF or TGF-α was detected in Reg IV-CM by ELISA. Taken together, these results suggest that Reg IV plays important roles in tumor progression and unfavorable prognosis. However, TGF-α positivity was also found more frequently in Tyr^{1068}-positive EGFR cases than in Tyr^{1068}-negative EGFR cases. Because frequency of Reg IV positivity in Tyr^{1068}-positive EGFR cases (67%) was lower than that of TGF-α positivity in Tyr^{1068}-positive EGFR cases (78%), EGFR phosphorylation may be due to the stimulation by TGF-α rather than Reg IV protein in PCa tissues.

Androgen-deprivation therapy has been used for decades in the treatment of prostate cancer.[20] Although this treatment is initially very effective in hormone-dependent cancers, they invariably become hormone-refractory and metastasize, resulting in death.[21] Novel therapies that target androgen-independent proliferation, as well as invasion and angiogenesis, may have enormous potential for improving the care of patients with advanced PCa. Several possible mechanisms by which PCa can escape the effects of androgen-deprivation therapy have been reported.[21] Among them, EGFR expression has been reported to be associated with hormone-refractory status.[22] Therefore, phosphorylation of the EGFR by Reg IV may participate in the acquisition of hormone-refractory status. In the present study, few tumor cells (1–10%) in clinically localized PCa showed Reg IV staining, although residual hormone-refractory PCa has been reported to express high levels of *REG4* mRNA.[11] These results suggest that Reg IV-positive tumor cells may escape the effects

doi: 10.1111/j.1349-7006.2008.00846.x
© 2008 Japanese Cancer Association

of androgen-deprivation therapy, resulting in an increased number of Reg IV-positive tumor cells in residual hormone-refractory PCa.

It has been reported that growth factors enhance *REG4* mRNA expression in colon cancer cells.[15] In fact, in PCa tissues, Reg IV positivity was found more frequently in TGF-α-positive cases than in TGF-α-negative cases. In contrast, neither EGF or TGF-α had any significant effect on Reg IV protein expression in LNCaP and DU145 cell lines, suggesting that, in addition to TGF-α, other factors are needed to express Reg IV in PCa cells.

In the present study, Reg IV-positive cases were frequently found in association with MUC2 positivity. It has been suggested that the acquisition by tumor cells of a mucinous phenotype, such as MUC2 expression, is involved in hormonal escape in PCa.[23] Reg IV-positive cases were frequently found in association with chromogranin A positivity. Neuroendocrine differentiation has been also reported to be correlated with tumor aggressiveness, short survival and poor response to androgen-deprivation therapy.[24,25] Therefore, Reg IV may be a key factor mediating the hormone-refractory phenotype in MUC2-positive or chromogranin A-positive PCa. We observed two Reg IV staining patterns, mucin-like staining and perinuclear staining. In gastric cancer, mucin-like Reg IV staining is associated with MUC2 positivity.[5] Perinuclear Reg IV staining is detected in cells with neuroendocrine differentiation and that show chromogranin A positivity. In PCa tissue, although almost all tumor cells showing mucin-like staining of Reg IV were positive for MUC2, some tumor cells showing perinuclear Reg IV staining also showed MUC2 staining. The significance of the difference between mucin-like Reg IV staining and perinuclear Reg IV staining is unclear; however, there were several PCa cases in which both staining patterns were observed and we presume that these staining patterns are not independent.

In conclusion, we showed that Reg IV immunostaining is an independent predictor of relapse-free survival in patients with clinically localized PCa. To clarify whether Reg IV immunostaining is useful for the identification of patients most likely to benefit from adjuvant treatment, the association between Reg IV staining and response to adjuvant therapies should be investigated. We also showed that Reg IV-CM induces EGFR phosphorylation. Because Reg IV expression is narrowly restricted in non-cancerous tissues, Reg IV may be a good therapeutic target for PCa.

Acknowledgments

This work was supported, in part, by Grants-in-Aid for Cancer Research from the Ministry of Education, Culture, Science, Sports and Technology of Japan; and from the Ministry of Health, Labor and Welfare of Japan. We thank Ms Emiko Hisamoto for excellent technical assistance and advice. This work was carried out with the kind cooperation of the Research Center for Molecular Medicine, Faculty of Medicine, Hiroshima University. We thank the Analysis Center of Life Science, Hiroshima University, for the use of their facilities.

References

1 Jemal A, Siegel R, Ward E, Murray T, Xu J, Thun MJ. Cancer statistics, 2007. *CA Cancer J Clin* 2007; **57**: 43–66.
2 D'Amico AV, Whittington R, Malkowicz SB *et al.* Clinical utility of the percentage of positive prostate biopsies in defining biochemical outcome after radical prostatectomy for patients with clinically localized prostate cancer. *J Clin Oncol* 2000; **18**: 1164–72.
3 Oue N, Hamai Y, Mitani Y *et al.* Gene expression profile of gastric carcinoma: identification of genes and tags potentially involved in invasion, metastasis, and carcinogenesis by serial analysis of gene expression. *Cancer Res* 2004; **64**: 2397–405.
4 Aung PP, Oue N, Mitani Y *et al.* Systematic search for gastric cancer-specific genes based on SAGE data: melanoma inhibitory activity and matrix metalloproteinase-10 are novel prognostic factors in patients with gastric cancer. *Oncogene* 2006; **25**: 2546–57.
5 Oue N, Mitani Y, Aung PP *et al.* Expression and localization of Reg IV in human neoplastic and non-neoplastic tissues: Reg IV expression is associated with intestinal and neuroendocrine differentiation in gastric adenocarcinoma. *J Pathol* 2005; **207**: 185–98.
6 Mitani Y, Oue N, Matsumura S *et al.* Reg IV is a serum biomarker for gastric cancer patients and predicts response to 5-fluorouracil-based chemotherapy. *Oncogene* 2007; **26**: 4383–93.
7 Isaacs W, De Marzo A, Nelson WG. Focus on prostate cancer. *Cancer Cell* 2002; **2**: 113–16.
8 Hasegawa Y, Matsubara A, Teishima J *et al.* DNA methylation of the RIZ1 gene is associated with nuclear accumulation of p53 in prostate cancer. *Cancer Sci* 2007; **98**: 32–6.
9 Oue N, Kuniyasu H, Noguchi T *et al.* Serum concentration of Reg IV in patients with colorectal cancer: overexpression and high serum levels of Reg IV are associated with liver metastasis. *Oncology*, 2007; **72**: 371–80.
10 Takehara A, Eguchi H, Ohigashi H *et al.* Novel tumor marker REG4 detected in serum of patients with resectable pancreatic cancer and feasibility for antibody therapy targeting REG4. *Cancer Sci* 2006; **97**: 1191–7.
11 Gu Z, Rubin MA, Yang Y *et al.* Reg IV: a promising marker of hormone refractory metastatic prostate cancer. *Clin Cancer Res* 2005; **11**: 2237–43.
12 Bishnupuri KS, Luo Q, Murmu N, Houchen CW, Anant S, Dieckgraefe BK. Reg IV activates the epidermal growth factor receptor/Akt/AP-1 signaling pathway in colon adenocarcinomas. *Gastroenterology* 2006; **130**: 137–49.
13 Yasui W, Ayhan A, Kitadai Y *et al.* Increased expression of p34cdc2 and its kinase activity in human gastric and colonic carcinomas. *Int J Cancer* 1993; **53**: 36–41.
14 Mantel N. Evaluation of survival data and two new rank order statistics arising in its consideration. *Cancer Chemother Rep* 1966; **50**: 163–70.
15 Nanakin A, Fukui H, Fujii S *et al.* Expression of the REG IV gene in ulcerative colitis. *Lab Invest* 2007; **87**: 304–14.
16 Cohen DW, Simak R, Fair WR, Melamed J, Scher HI, Cordon-Cardo C. Expression of transforming growth factor-alpha and the epidermal growth factor receptor in human prostate tissues. *J Urol* 1994; **152**: 2120–4.
17 Culig Z, Hobisch A, Cronauer MV *et al.* Regulation of prostatic growth and function by peptide growth factors. *Prostate* 1996; **28**: 392–405.
18 Connolly JM, Rose DP. Angiogenesis in two human prostate cancer cell lines with differing metastatic potential when growing as solid tumors in nude mice. *J Urol* 1998; **160**: 932–6.
19 Bonaccorsi L, Carloni V, Muratori M *et al.* EGF receptor (EGFR) signaling promoting invasion is disrupted in androgen-sensitive prostate cancer cells by an interaction between EGFR and androgen receptor (AR). *Int J Cancer* 2004; **112**: 78–86.
20 Huggins C. Endocrine-induced regression of cancers. *Science* 1967; **156**: 1050–4.
21 Feldman BJ, Feldman D. The development of androgen-independent prostate cancer. *Nat Rev Cancer* 2001; **1**: 34–45.
22 Shah RB, Ghosh D, Elder JT. Epidermal growth factor receptor (ErbB1) expression in prostate cancer progression: correlation with androgen independence. *Prostate* 2006; **66**: 1437–44.
23 Legrier ME, de Pinieux G, Boye K *et al.* Mucinous differentiation features associated with hormonal escape in a human prostate cancer xenograft. *Br J Cancer* 2004; **90**: 720–7.
24 McWilliam LJ, Manson C, George NJ. Neuroendocrine differentiation and prognosis in prostatic adenocarcinoma. *Br J Urol* 1997; **80**: 287–90.
25 di Sant'Agnese PA, Cockett AT. Neuroendocrine differentiation in prostatic malignancy. *Cancer* 1996; **78**: 357–61.

© 2008 Japanese Cancer Association

Protection of telomeres 1 protein levels are associated with telomere length in gastric cancer

KIYOMU FUJII[1], TOMONORI SASAHIRA[1], YUKIKO MORIWAKA[1], NAOHIDE OUE[2], WATARU YASUI[2] and HIROKI KUNIYASU[1]

[1]Department of Molecular Pathology, Nara Medical University School of Medicine, Kashihara, Nara; [2]Department of Molecular Pathology, Hiroshima University Graduate School, Hiroshima, Japan

Received December 3, 2007; Accepted January 25, 2008

Abstract. Protection of telomeres 1 (Pot1) is a telomere-associated protein, which binds to the single-stranded DNA extensions of telomeres and regulates telomere length. Pot1 production was examined and compared with telomere length in gastric cancer. Pot1 production and telomere lengths were assessed in 5 human gastric cancer cell lines by immunoblotting and Southern blotting, respectively. Pot1 intracellular localization was examined with protein fractionation. Pot1 index and telomere volume were examined in human gastric mucosa and cancer by immunohistochemistry and *in situ* hybridization. Pot1 protein levels, which were lower than those in the lymphocytes of healthy persons, were significantly correlated with telomere length in gastric cancer cells (P=0.0167). Pot1 protein was mainly detected in the nuclear fraction and increased by G2/M blocking with nocodazole in MKN28 cells. Pot1 indexes were correlated with telomere volumes in gastric cancers (P<0.0001). Pot1 index was decreased in gastric epithelia distant from cancer (84±14%), in peritumoral epithelia (72±24%), and in stage I-II (39±14%) and stage III-IV (23±14%) gastric cancers (P<0.0001). Pot1 index was lower in stage III-IV than in stage I-II gastric cancers (P<0.05). Pot1-low cases showed advanced cancer invasion (P<0.05). Thus, Pot1 production was closely associated with telomere length in gastric mucosa and cancers. Pot1 might be a good *in situ* marker for the examination of cell-specific telomere length.

Correspondence to: Dr Hiroki Kuniyasu, Department of Molecular Pathology, Nara Medical University School of Medicine, 840 Shijo-cho, Kashihara, Nara 634-8521, Japan
E-mail: cooninh@zb4.so-net.ne.jp

Abbreviations: Pot1, protection of telomeres 1; *H. pylori*, *Helicobactor pylori*; hTERT, human telomerase reverse transcriptase; hTR, human telomerase RNA

Key words: telomere, telomere length, gastric cancer

Introduction

The telomere is a repetitive sequence of TTAGGG, located at the chromosomal ends. Telomere reduction is closely associated with aging, inflammatory, regenerative, and carcinogenic processes in various cells and tissues (1-4). In our previous study, the telomeres were reduced at various levels in the epithelial cells in the gastric mucosa in comparison with mucosa-infiltrating lymphocytes, smooth muscle cells, and endothelial cells (5). In particular, telomeres were notably reduced in the intestinal metaplasia epithelium with *Helicobactor pylori* (*H. pylori*) infection, in which human telomerase reverse transcriptase (hTERT) protein expression was found in association with a marked reduction of telomeres (5). Human telomerase RNA (hTR) is also expressed in relation to *H. pylori* infection in intestinal metaplasia (6). Telomere shortening, expression of hTR and hTERT, and telomerase activation are commonly found in gastric cancer (7). From these findings, we can hypothesize that the earliest stage of gastric cancer development might be associated with telomere reduction.

Protection of telomeres 1 (Pot1) is a telomere-associated protein, which is isolated from ciliated protozoa (8). Pot1 binds to the single-stranded G-rich DNA extensions of the telomere with its N-terminal DNA-binding domain, and protects the chromosomal ends from chromosomal instability (8,9). Pot1 localizes to telomeres in the interphase nuclei of human cells (10) or during periods of the cell cycle when t-loops are thought to be present (11). Pot1 regulates the telomere length: TRF1 regulates Pot1-binding with single-strand telomere DNA and Pot1 controls telomerase-mediated telomere elongation by *cis*-inhibition of telomerase (12-14). We previously reported that 3' telomeric overhang signals decreased in accordance with decreases in Pot1 expression levels and telomere shortening (15). In gastric cancer, the mRNA expression of *Pot1* is associated with telomere length and cancer progression (15,16).

In the present study, we demonstrated that Pot1 protein level were closely associated with telomere length in gastric cancer cells and were decreased in gastric mucosal epithelia and gastric cancer.

Materials and methods

Cell culture. Human gastric cancer cell lines, MKN28, MKN45, TMK1, HSC39 were routinely maintained in RPMI-1640 (Sigma Chemical Co., St. Louis, MO) containing 10% fetal bovine serum (FBS, Sigma Chemical Co.) under the conditions of 5% CO_2 in air at 37°C. Lymphocytes used as the control for Pot1 expression and telomere length were obtained from the peripheral blood of 3 healthy volunteers, whose mean age was matched to gastric cancer patients (2 men and 1 woman, 59, 61 and 65 years of age, mean: 61.7 years). Lymphocytes ($1x10^7$) were collected from each volunteer and mixed for examination.

Patients and tumor specimens. Twenty-four gastric cancer patients (12 stage I-II and 12 stage III-IV cases; 15 men and 9 women, 52-78 years of age, mean: 63.6 years) were randomly selected from the cases analyzed in our previous study (5). A formalin-fixed, paraffin-embedded surgical specimen containing the deepest invasion site was chosen from the tissue specimens of each patient. Tumor staging and histopathological grading were classified according to the UICC TNM classification system (17) and Lauren's classification (18). Their medical records and prognostic follow-up data were obtained from the patient database maintained by the hospital.

Immunoblot analysis. Whole-cell lysates were prepared as described previously (19). Fifty-microgram lysates were subjected to immunoblot analysis in 12.5% sodium dodecyl sulfate-polyacrylamide gels followed by electrotransfer onto nitrocellulose filters. The filters were incubated with primary antibodies and then with peroxidase-conjugated IgG antibodies (Medical and Biological Laboratories, Nagoya, Japan). An α-tubulin antibody was used to assess the levels of protein loaded per lane (Oncogene Research Products, Cambridge, MA). The immune complex was visualized by a CSA system (Dako, Carpinteria, CA). Anti-protection of telomeres 1 (Pot1) antibodies (Santa Cruz Biotechnology, Santa Cruz, CA) were used as the primary antibodies.

Southern blot analysis. High molecular weight genomic DNA was extracted with a DNA Extraction Kit (Stratagene Cloning System, La Jolla, CA). DNA was digested with *Hin*fI (Takara Biomedicals, Tokyo, Japan), electrophoresed on 0.8% agarose-TAE gels, and blotted onto nitrocellulose filters. The filters were hybridized with $(TTAGGG)_4$ probe labeled with biotin at the 5' end (Sigma Genosys, Ishikari, Japan), which was detected with peroxidase-conjugated avidine and visualized with an ECL system (both from Dako). We estimated the telomere length as the peak signal using Kodak Digital Science 1D software (Eastman Kodak Company, New Haven, CT). DNA ladders (2.5-kb and 1-kb) (Takara Biomedicals) were used for the measurement of peak telomere length.

Intracellular localization. MKN28 cells grown in culture dishes were treated with or without nocodazole (Alexis Biochemicals, San Diego, CA; 100 ng/ml for 24 h). The cells were re-suspended in 500 μl of STKM buffer [50 mM Tris HCl pH 7.5, 25 mM KCl, 5 mM $MgCl_2$, 0.25 M sucrose, 10 μg/ml leupeptin, 50 μg/ml phenylmethylsulfonyl fluoride (PMSF)] and stroked 150 times in dounce pestles. After a 1,000 x g, 5-min centrifugation, the supernatant was centrifugated at 40,000 x g for 1 h at 4°C to separate the membrane fraction (pellet) and the cytosol fraction (supernatant). The pellet was re-suspended by 1000 x g-spin into hypertonic buffer (25 mM Tris HCl pH 7.8, 10 mM KCl, 5 mM $MgCl_2$, 10 μg/ml leupeptin, 50 μg/ml PMSF) and incubated for 5 min on ice followed by the addition of the same amount of 2X STKM buffer. After centrifugation at 40,000 x g for 1 h at 4°C, the pellet was re-suspended with nuclear extraction buffer (20 mM Hepes pH 7.9, 420 mM NaCl, 1.5 mM $MgCl_2$, 0.2 mM EDTA, 0.5 mM DTT, 25% glycerol) as the nuclear fraction. Loading amounts were monitored by Coomassie blue staining of the same amount of the proteins dot-blotted onto nitrocellulose membrane.

Immunohistochemistry. Immunohistochemistry was performed as previously described (20). Sections (4 μm thick) of each specimen were mounted on ProbeOn slides for ISH (Fisher Scientific, Pittsburgh, PA). An immunoperoxidase technique was used following antigen retrieval with microwave (1,000 W) treatment for 10 min three times in citrate buffer (pH 6.0). After blocking endogenous peroxidase activity with 3% H_2O_2-methanol for 15 min, the specimens were rinsed with phosphate-buffered saline (PBS). Anti-Pot1 antibody (Santa Cruz Biotechnology) diluted to 0.5 μg/ml was used as the primary antibody. After a 2-h incubation at room temperature, the slides were rinsed with PBS and incubated at room temperature for 1 h with a secondary antibody conjugated to peroxidase (1:200) (anti-goat IgG antibody, Medical and Biological Laboratories Co. Ltd). After being rinsed with PBS, all specimens were color-developed with diaminobenzidine (DAB) solution (Dako). Immunostaining of all specimens was performed simultaneously to ensure the same antibody reaction and DAB exposure conditions. Nuclear immunoreactivity was judged as positive. Pot1 positivity was examined as follows: 1,000 nuclei were observed in Pot1 immunostained slides under x200 magnification microscopy. The Pot1 index was designated as a percentage. Data of telomere volume in gastric cancer cases were derived from our previous study (5).

Telomere volume. Telomere volume was determined by fluorescent *in situ* hybridization (FISH). Sections (10 μm thick) of each specimen were mounted on ProbeOn slides (Fisher Scientific, Pittsburgh, PA) for ISH. The telomere repeat probe $(TTAGGG)_4$ was labeled with fluorescein isothiocyanate (FITC) on the 3'-tail (EspecOligo Service, Tsukuba, Japan) (5). The probe was diluted to 20 μg/ml by probe hybridization solution [50% formamide (Sigma Chemical Co.), 0.5 M NaCl, 5% polyethylene glycol 8000 [Sigma Chemical Co.)]. The specimens were dewaxed and dehydrated with xylene and 100% ethanol. They were then hydrated in Tris-buffered saline (Sigma Chemical Co.) and digested with 0.2% pepsin-2 M HCl (Dako) for 1 h at 37°C, and then subjected to RNase A (10 μg/μl, Takara Biomedicals) treatment at 37°C for 10 min. Specimens were then heated with probe solution at 100°C for 5 min, cooled to 4°C for

Table I. Pot1 protein levels and telomere length in gastric carcinoma cell lines.

Cell line	Pot1 level (%)[a]	Telomere length (kb)
MKN28	47	4.7
MKN45	42	3.8
TMK1	31	3.1
HSC39	25	2.8
Lymphocytes	100	9.9

[a]Signal density of immunoblotting was standardized with that in lymphocytes, which was set to 100%.

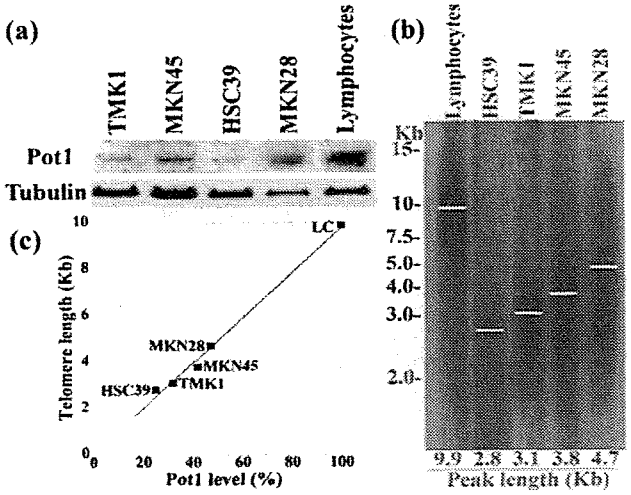

Figure 1. Pot1 production and telomere length in human gastric cancer cell lines. (a) Pot1 production was detected by immunoblotting in gastric cancer cells. Lymphocytes were examined as the normal control. Tubulin was detected as the loading control. (b) Telomere length was examined by Southern blot analysis in gastric cancer cells. Peak length is designated by a white line in each lane. (c) Correlation between Pot1 production and telomere length was examined. Pot1 production was designated as a percentage of that in lymphocytes (LC).

15 min, and then maintained at 37°C for 2 h. The specimens were rinsed five times with 1X standard sodium chloride/ sodium citrate at 45°C.

Specimens hybridized with the $(TTAGGG)_4$ probe were examined with 520-nm light for FITC. Specimen images were stored on a computer and processed (Fig. 1a). Briefly, 100 nuclei were identified from the images, and the hybridization signals were scanned as inverted gray-scale images by means of NIH Image software (National Institute for Health, Bethesda, MD). The mean signal density and mean nuclear area of the 100 nuclei were calculated. The mean density was divided by the mean nuclear area (μm^2) to adjust for differences in the DNA amounts of the identified nuclei. The resulting value was considered to be representative of the telomere density of the tissue and was termed telomere volume to distinguish it from the telomere length determined by Southern blot analysis (5).

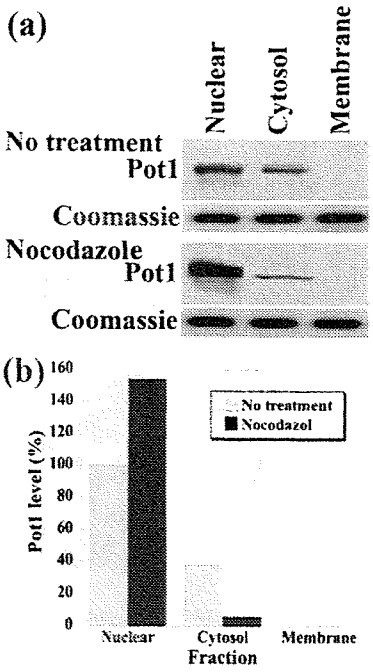

Figure 2. Intracellular localization of Pot1 was examined using fractionated protein extraction of MKN28 gastric cancer cells. (a) Pot1 was detected in each protein fraction by immunoblotting. Loading amounts were monitored by Coomassie blue staining of the same amount of protein dot-blotted onto nitrocellulose membrane. To increase G2/M phase cells, MKN28 cells were treated with nocodazole (100 ng/ml, 24 hrs). (b) Relative Pot1 protein levels. Pot1 level in the nuclear fraction of untreated cells was set to 100%.

Statistical analysis. Statistical significance was examined by the Spearman's Rank test, the two-tailed, unpaired Mann-Whitney U test, and Fisher's exact test using InStat software (Graphpad Software, Los Angeles, CA). Statistical significance was defined as a two-sided P-value of <0.05.

Results

Pot1 production and telomere length in gastric cancer cells (Table I). We first examined Pot1 protein production in gastric carcinoma cells (Fig. 1a). Pot1 expression in gastric cancer cells was decreased in comparison with human lymphocytes. The telomere lengths of these cells were next examined (Fig. 1b). The gastric cancer cell lines showed reduced telomere length in comparison with the lymphocytes of healthy persons. We compared Pot1 expression with telomere length in the cells (Fig. 1c). Pot1 production was significantly correlated with telomere length (Spearman R=0.9998, P=0.0167).

Intracellular localization of Pot1 in gastric cancer cells. Next, the intracellular localization of Pot1 was examined in MKN28 cells (Fig. 2). In untreated MKN28 cells, Pot1 protein was detected in the nuclear and cytosol fraction. Pot1 was not detected in the membrane fractions. When MKN28 cells were treated with nocodazole to stop the cell cycle at G2/M phase, Pot1 was increased in the nuclear fraction, whereas it was decreased in the cytosol fraction.

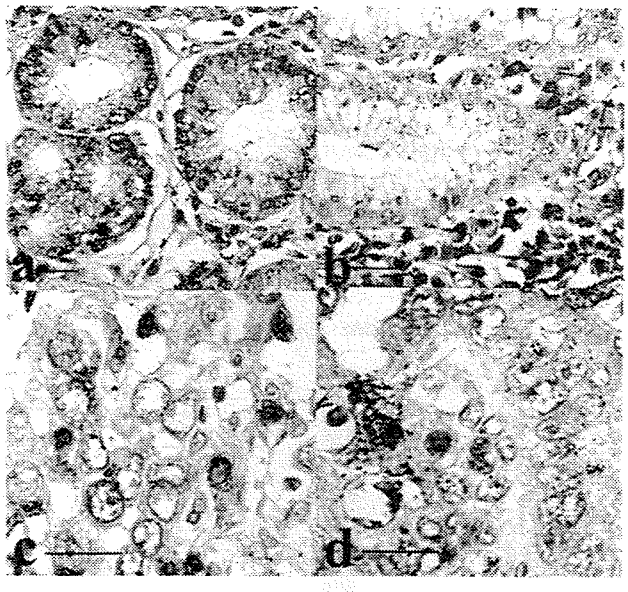

Figure 3. Immunohistochemistry of Pot1 in gastric mucosa and cancer. (a) Gastric mucosa distant from the tumor. (b) Peritumoral mucosa. (c) Early-stage gastric cancer. (d) Advanced gastric cancer. Nuclear immunoreactivity was judged as positive. Bar, 50 μm.

Table II. Pot1 positivity and telomere volume in human gastric cancer.

Case no.	Pathological stage	Pot1 positivity (%)	Telomere volume (%)
1	I	58	68
2	I	54	65
3	I	52	41
4	I	47	76
5	I	45	62
6	I	42	52
7	I	40	58
8	I	31	71
9	II	25	33
10	II	18	52
11	II	16	42
12	III	48	60
13	III	43	65
14	III	38	70
15	III	33	52
16	III	30	21
17	III	24	25
18	III	24	47
19	III	18	35
20	IV	12	43
21	IV	10	18
22	III	8	33
23	IV	8	23
24	IV	5	23

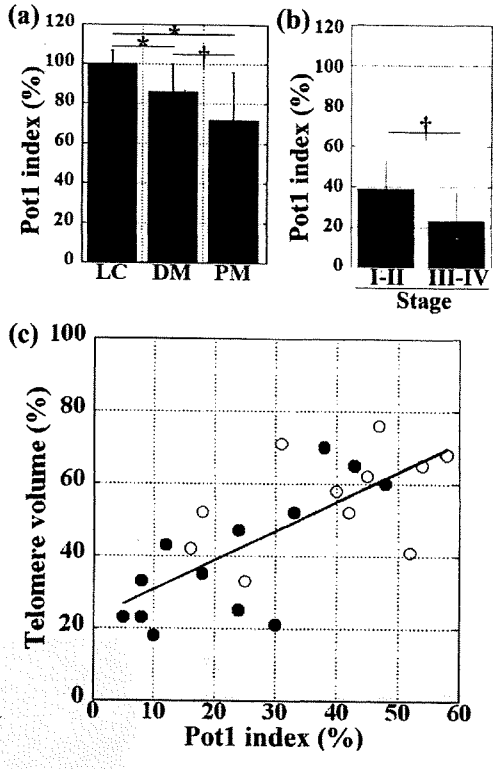

Figure 4. Pot1 positivity and telomere volume in human gastric mucosa and cancer. (a) Pot1 positivity in: lymphocytes (LC), mucosa distant from the tumor (DM), peritumoral mucosa (PM). (b) Pot1 positivity in stage I-II and stage III-IV cases. *P<0.0005, †P<0.05; error bar, SD. (c) Correlation between Pot1 positivity and telomere volume in gastric carcinomas. Telomere volume was designated as a percentage of that in lymphocytes. ○, stage I-II; ●, stage III-IV. Spearman R=0.7137, P<0.0001.

Immunohistochemistry of Pot1 in gastric mucosa and cancer. The Pot1 index was examined in non-cancerous gastric mucosa by immunohistochemistry (Fig. 3a and b). In mucosal epithelial cells distant from the tumors, the Pot1 index was reduced to 84±14% of that in the infiltrating lymphocytes (P=0.0003, Fig. 3a and Fig. 4a). In contrast, the Pot1 index was more reduced in the epithelial cells in the peritumoral mucosa (within 5 mm from the tumoral periphery), to 72±24% of that in the infiltrating lymphocytes (P=0.0001, Fig. 3b and Fig. 4a). The Pot1 index was significantly lower in the epithelial cells in the peritumoral mucosa than those in the mucosa distant from the tumors (P<0.05).

Next, the Pot1 index was examined in cancer tissues by immunohistochemistry (Fig. 3c and d, Table II). In Stage I-II gastric cancer, the Pot1 index was reduced to 39±14% of that in the infiltrating lymphocytes (P<0.0001, Fig. 4b). It was more reduced in Stage III-IV gastric cancer, to 23±14% of that in the infiltrating lymphocytes (P<0.0001, Fig. 4b). Pot1 positivity was significantly lower in stage III-IV cancers than in stage I-II cancers (P<0.05). We compared Pot1 positivity and telomere volume in the cases (Fig. 4c). The two parameters were significantly correlated in a linear regression manner (Spearman R=0.7137, P<0.0001).

Finally, we compared the Pot1 index and clinicopathological parameters (Table III). The 24 gastric cancer cases were divided into two groups by Pot1 index: Pot1-low (12 cases with lower Pot1 index) and Pot1-high (12 cases with higher

Table III. Comparison of Pot1 index with clinicopathological parameters in 24 gastric cancer cases.

	Pot1 high (n=12)	Pot1 low (n=12)	P
Pot1 index (%)	31-58 (median 44) 44.3±8.2	5-30 (median 17) 16.5±8.0	<0.0001
Telomere volume (%)[a]	41-76 (median 63.5) 61.7±9.8	18-52 (median 33) 32.9±11.2	0.0001
Age (years)	48-81 (median 64) 64.0±9.9	43-78 (median 66.5) 63.8±11.3	NS
Gender (M:F)	7:5	7:5	NS
Pathological stage[b] (I-II vs III-IV)	7:4	4:8	NS
T-factor[b] (T1-T2:T3)	11:1	5:7	<0.0500
N-factor[b] (N0:N1-N2)	6:6	4:8	NS
M-factor[b] (M0:M1)	12:0	9:3	NS
Histology[c] (intestinal vs diffuse type)	8:4	5:7	NS

[a]Telomere volume was examined by fluorescent *in situ* hybridization using $(TTAGGG)_4$ probe. [b]Pathological staging, T-factor, N-factor, and M-factor (all positive cases showed peritoneal dissemination in this study) were defined according to the TNM classification system (17). [c]Histological classification was done according to Lauren's classification (18). NS, not significant.

Pot1 index). The Pot1 indexes of Pot1-low and Pot1-high groups were 16.5±8.0% and 44.3±8.2%, respectively (P<0.0001). The telomere volumes in the Pot1-high group were higher (61.7±9.8%) than those in the Pot1-low group (32.9±11.2%) (P=0.0001).There was no difference between the two groups in age, gender, pathological stage, N-factor (nodal metastasis), M-factor (peritoneal dissemination), and histological types; however, T-factor (invasive depth) was advanced in Pot1-low. The number of T3 cases (invading the serosa) was 7 out of 12 (58%) in the Pot1-low group, and, in contrast, 1 out of 12 (8%) in the Pot1-high group (P<0.05).

Discussion

We confirmed that Pot1 expression was closely correlated with telomere length in gastric cancer cells and human lymphocytes. Pot1 was localized to the t-loops of telomeres in the interphase nuclei of human cells (10,11). We confirmed Pot1 intracellular localization by the fractionated cellular proteins. Pot1 was found in the nuclear and cytosol fractions in MKN28 cells cultured in regular conditions, whereas it was mainly found in the nuclear fraction in nocodazole-treated MKN28 cells, whose cell cycle was stopped at G2/M. This observation suggests that Pot1 might be recruited into the nuclei in the G2/M phase to bind to telomeres. The Pot1 localization detected by immunohistochemistry was found in whole nuclei or the nuclear periphery. This is similar to that of the telomeres in our previous observations (5), which suggests the co-localization of Pot1 and telomeres.

Immunohistochemical examination of the Pot1 index in gastric mucosa and cancer showed that it was reduced in gastric epithelia and gastric cancer in comparison with infiltrated lymphocytes. Cancer cells showed a lower Pot1 index than gastric epithelia. To confirm the relationship of Pot1 positivity with telomere reduction, we compared Pot1 positivity and our previous data for telomere volume in the same cases (5). The results showed significant correlation between the two parameters and suggest that Pot1 expression corresponds to telomere length in the cells or tissues.

Notably, the Pot1 index was significantly lower in the gastric epithelium adjacent to the tumoral periphery than in epithelia distant from the tumor. Two possibilities are proposed. One is that it was affected by the tumor: the mucosa adjacent to colon cancer showed hyperplastic, proliferative, and angiogenic properties, which were responses to the growth factors and cytokines produced by cancer cells (21). Another is that it is a precancerous change leading to gastric cancer. Telomere reduction is a strong stimulus for the reactivation of telomerase in somatic cells and is associated with carcinogenic processes in many cancers (3,22). Pot1 decrease might be associated with telomerase activation and hence with the transformation of gastric epithelia. In further study, we will endeavour to detect early-stage gastric cancer by examining Pot1 expression as a probe.

Acknowledgments

This work was supported in part by a Grant-in-Aid for Scientific Research (C) from the Japan Society for the Promotion of Science, Japan.

References

1. Harley CB: Human aging and telomeres. Ciba Found Symp 211: 129-139, 1997.

2. Greider CW and Blackburn EH: Telomeres, telomerase and cancer. Sci Am 274: 92-97, 1996.
3. Holt SE, Wright WE and Shay JW: Multiple pathways for the regulation of telomerase activity. Eur J Cancer 33: 761-766, 1997.
4. Weng NP, Palmer LD, Levine BL, Lane HC, June CH and Hodes RJ: Tales of tails: regulation of telomere length and telomerase activity during lymphocyte development, differentiation, activation, and aging. Immunol Rev 160: 43-54, 1997.
5. Kuniyasu H, Kitadai Y, Mieno H and Yasui W: *Helicobactor pylori* infection is closely associated with telomere reduction in gastric mucosa. Oncology 65: 275-282, 2003.
6. Kuniyasu H, Domen T, Hamamoto T, Yokozaki H, Yasui W, Tahara H and Tahara E: Expression of human telomerase RNA is an early event of stomach carcinogenesis. Jpn J Cancer Res 88: 103-107, 1997.
7. Tahara H, Kuniyasu H, Yokozaki H, Yasui W, Shay JW, Ide T and Tahara E: Telomerase activity in preneoplastic and neoplastic gastric and colorectal lesions. Clin Cancer Res 1: 1245-1251, 1995.
8. Baumann P and Cech TR: Pot1, the putative telomere end-binding protein in fission yeast and humans. Science 292: 1171-1175, 2001.
9. Lei M, Baumann P and Cech TR: Cooperative binding of single-stranded telomeric DNA by the Pot1 protein of *Schizosaccharomyces pombe*. Biochemistry 41: 14560-14568, 2002.
10. Baumann P, Podell E and Cech TR: Human Pot1 (protection of telomeres) protein: cytolocalization, gene structure, and alternative splicing. Mol Cell Biol 22: 8079-8087, 2002.
11. Wei C and Price CM: Cell cycle localization, dimerization, and binding domain architecture of the telomere protein cPot1. Mol Cell Biol 24: 2091-2102, 2004.
12. Loayza D and De Lange T: POT1 as a terminal transducer of TRF1 telomere length control. Nature 423: 1013-1018, 2003.
13. Colgin LM, Baran K, Baumann P, Cech TR and Reddel RR: Human POT1 facilitates telomere elongation by telomerase. Curr Biol 13: 942-946, 2003.
14. Ye JZ, Hockemeyer D, Krutchinsky AN, Loayza D, Hooper SM, Chait BT and De Lange T: POT1-interacting protein PIP1: a telomere length regulator that recruits POT1 to the TIN2/TRF1 complex. Genes Dev 18: 1649-1654, 2004.
15. Kondo T, Oue N, Yoshida K, Mitani Y, Naka K, Nakayama H and Yasui W: Expression of POT1 is associated with tumor stage and telomere length in gastric carcinoma. Cancer Res 64: 523-529, 2004.
16. Lin X, Gu J, Lu C, Spitz MR and Wu X: Expression of telomere-associated genes as prognostic markers for overall survival in patients with non-small cell lung cancer. Clin Cancer Res 12: 5720-5725, 2006.
17. Sobin LH and Wittekind C (eds): UICC TNM Classification of Malignant Tumours. 6th edition, John Wiley & Sons Inc., New York, 2003.
18. Lauren P: The two histological main types of gastric carcinoma: diffuse and so-called intestinal-type carcinoma. An attempt at a histo-clinical classification. Acta Pathol Microbiol Scand 64: 31-49, 1965.
19. Kuniyasu H, Yasui W, Kitahara K, Naka K, Yokozaki H, Akama Y, Hamamoto T, Tahara H and Tahara E: Growth inhibitory effect of interferon-beta is associated with the induction of cyclin-dependent kinase inhibitor p27Kip1 in a human gastric carcinoma cell line. Cell Growth Differ 8: 47-52, 1997.
20. Kuniyasu H, Oue N, Wakikawa A, Shigeishi H, Matsutani N, Kuraoka K, Ito R, Yokozaki H and Yasui W: Expression of receptors for advanced glycation end-products (RAGE) is closely associated with the invasive and metastatic activity of gastric cancer. J Pathol 196: 163-170, 2002.
21. Kuniyasu H, Yasui W, Shinohara H, Yano S, Ellis LM, Wilson MR, Bucana CD, Rikita T, Tahara E and Fidler IJ: Induction of angiogenesis by hyperplastic colonic mucosa adjacent to colon cancer. Am J Pathol 157: 1523-1535, 2000.
22. Greider CW: Telomere length regulation. Annu Rev Biochem 65: 337-365, 1996.

nature genetics

© 2008 Nature Publishing Group http://www.nature.com/naturegenetics

Genetic variation in *PSCA* is associated with susceptibility to diffuse-type gastric cancer

The Study Group of Millennium Genome Project for Cancer*

Gastric cancer is classified into intestinal and diffuse types, the latter including a highly malignant form, linitis plastica. A two-stage genome-wide association study (stage 1: 85,576 SNPs on 188 cases and 752 references; stage 2: 2,753 SNPs on 749 cases and 750 controls) in Japan identified a significant association between an intronic SNP (rs2976392) in *PSCA* (prostate stem cell antigen) and diffuse-type gastric cancer (allele-specific odds ratio (OR) = 1.62, 95% CI = 1.38–1.89, $P = 1.11 \times 10^{-9}$). The association was far less significant in intestinal-type gastric cancer. We found that *PSCA* is expressed in differentiating gastric epithelial cells, has a cell-proliferation inhibition activity *in vitro* and is frequently silenced in gastric cancer. Substitution of the C allele with the risk allele T at a SNP in the first exon (rs2294008, which has $r^2 = 0.995$, $D' = 0.999$ with rs2976392) reduces transcriptional activity of an upstream fragment of the gene. The same risk allele was also significantly associated with diffuse-type gastric cancer in 457 cases and 390 controls in Korea (allele-specific OR = 1.90, 95% CI = 1.56–2.33, $P = 8.01 \times 10^{-11}$). The polymorphism of the *PSCA* gene, which is possibly involved in regulating gastric epithelial-cell proliferation, influences susceptibility to diffuse-type gastric cancer.

Gastric cancer, the fourth most common cancer and the second leading cause of cancer death in the world, has an incidence and mortality particularly high in Japan and Korea[1,2]. Histopathological research has long suggested that gastric cancer is not a single disease and recognizes two major categories: intestinal and diffuse[1,3,4]. (**Supplementary Table 1** online). Besides their morphological differences, the two types may also be distinct in their pathogenesis.

The intestinal type predominates in high-risk geographic areas such as East Asia, showing a correlation with the prevalence in the region of *Helicobacter pylori* infection among the elderly. Typically, intestinal-type gastric cancer arises through a sequence of events: *H. pylori*–induced persistent inflammation, hypochlorhydria, atrophic gastritis, intestinal metaplasia and intestinal-type adenocarcinoma.

The diffuse type, however, is more uniformly distributed geographically, is apparently unrelated to *H. pylori* prevalence[1] and typically develops from *H. pylori*–free, morphologically normal gastric mucosa without atrophic gastritis or intestinal metaplasia. Unlike the decreasing incidence of the intestinal type, the prevalence of the diffuse type is reportedly increasing worldwide[1].

The intestinal and diffuse types show histological characteristics of well- and poorly differentiated adenocarcinomas, respectively, yet both can coexist in the same gastric cancer tissue specimen, which suggests that a degradation of a well-differentiated glandular architecture to a poorly differentiated morphology may occur in some cases during cancer development[5]. Such divergence may be mediated by somatic loss of *CDH1* function[6] and illustrates another example of the complexity in understanding the initial carcinogenesis mechanisms through the morphological features of the advanced stage of the cancer. Nevertheless, a *de novo* diffuse-type gastric cancer is believed to exist and develop from stem cells or precursors for gastric epithelial cells in the background of relatively normal gastric mucosa[4,7].

Notably, advanced diffuse-type gastric cancer includes a distinct form of gastric cancer with an extremely poor prognosis: linitis plastica[8] (**Supplementary Fig. 1** online). This cancer accounts for about 10% of all gastric cancer, and its 5-year survival rate is around 10–20% in Japan[9]. Unlike the intestinal types, the diffuse types, including linitis plastica, occur almost equally among males and females, and linitis plastica shows a relative predominance in younger individuals[8,10,11].

Close to 100 pedigrees with an autosomal-dominant hereditary form of diffuse-type gastric cancer showed germline mutations of the *CDH1* gene. However, the pathogenic *CDH1* mutation seems to be rare among Japanese individuals with familial gastric cancer[12]. A large-scale twin study in northern Europe, where *H. pylori* prevalence is relatively low, estimated that heritability accounts for 28% of the variation in susceptibility to gastric cancer[13], but data specific to diffuse- or intestinal-type cancers were not available. Despite suggestions that intestinal- and diffuse-type gastric cancers develop through different carcinogenic pathways and that genetic background is more important in the latter[14], information on the genetic susceptibility factors specific to the diffuse type is scarce[15]. This study aims to identify genetic factors influencing predisposition to the sporadic form of diffuse-type gastric cancer, which may constitute a distinct disease entity and should be analyzed separately from intestinal-type gastric cancer.

*A full list of the authors appears at the end of this paper.

Received 6 December 2007; accepted 26 March 2008; published online 18 May 2008; doi:10.1038/ng.152

Table 1 Ten SNPs with the smallest *P* values for allele model odds ratio in the stage 2 screening

SNP ID				Stage 2 screening				Stage 1 screening		
IMS-JST	rs number	Chr.	Gene	OR	95% CI	Fisher	Permutation	OR	95% CI	Fisher
089945	rs2976392	8q24.3	*PSCA*	1.62	1.38–1.89	1.1×10^{-9a}	2.3×10^{-5}	1.89	1.45–2.46	1.2×10^{-6}
003203	rs2075570	1q22	*MTX1*	1.65	1.34–2.02	9.2×10^{-7a}	0.0020	1.70	1.20–2.40	0.0025
005799	rs2070803	1q22	*TRIM46*	1.62	1.33–1.98	1.2×10^{-6a}	0.0026	1.68	1.20–2.35	0.0022
163807	rs3804775	3q12.3	*PCNP*	1.32	1.14–1.54	2.4×10^{-4}	0.31	0.74	0.59–0.93	0.010
136603	rs301451	9p24.2	*C9orf68*	0.67	0.54–0.84	2.5×10^{-4}	0.31	1.47	1.03–2.10	0.032
089943	rs2976391	8q24.3	*PSCA*	1.42	1.17–1.72	3.2×10^{-4}	0.37	1.90	1.34–2.70	1.7×10^{-4}
047367	rs2244163	8q24.3	*LY6K*	1.41	1.16–1.72	4.3×10^{-4}	0.45	1.90	1.33–2.73	2.9×10^{-4}
060142	rs2303474	3q12.3	*ZBTB11*	1.30	1.12–1.51	5.4×10^{-4}	0.52	0.70	0.55–0.89	0.0032
089950	rs2585174	8q24.3	*LY6K*	1.31	1.12–1.53	6.5×10^{-4}	0.58	1.62	1.25–2.09	2.2×10^{-4}
044453	rs2291905	3q13.2	-	0.72	0.59–0.89	0.0017	0.86	1.53	1.07–2.19	0.020

Listed are the gene nearest to the SNP, the allelic odds ratio (major allele/minor allele), the 95% confidence interval and *P* values obtained by Fisher's exact test or by permutation test. Please note that SNPs were selected in the first screening not only by allele model, but also by considering dominant and recessive models. Twenty-six pairs and a trio in the total 940 samples showed high concordance in the genotype data. See Methods for details. [a]Statistically significant after Bonferroni adjustment ($P < 1.8 \times 10^{-5}$).

A genome-wide association study was conducted on the basis of the JSNP database (see URLs section in Methods), which catalogs the gene-centric SNPs ascertained from Japanese individuals[16,17]. This study is a part of a five-disease collaborative national project in Japan, in which two-stage genome-wide association studies on 100,000 JSNPs were simultaneously done for Alzheimer's disease, gastric cancer, type 2 diabetes, hypertension and asthma[18,19].

The genome scan identified a SNP in *PSCA* to be associated with the diffuse type of gastric cancer even after Bonferroni correction of multiple testing. PSCA was first identified as a prostate-specific antigen overexpressed in prostate cancers[20,21], but it was also expressed in the bladder, esophagus and stomach[22].

To fortify the observed statistical association, we carried out several analyses to assess the functional significance of the gene. Taken together, our findings suggest that *PSCA* has a role in proliferation of differentiating gastric epithelial cells, and that variation in the regulatory region of *PSCA* influences its expression, which might be translated to a predisposition to the diffuse type of gastric cancer.

RESULTS

SNPs in *PSCA* highly related to diffuse-type gastric cancer

The design, positive predictive value and sensitivity of our JSNP genome scan have been described previously[23]. In the first stage of the scan, genotype data at 85,576 SNPs on 188 cases and 752 controls passed a quality check. The 752 control samples were a mixture of Japanese individuals ascertained for one of four diseases—Alzheimer's disease, type 2 diabetes, hypertension and asthma—in the joint JSNP genome scan project[18] (see Methods). For the second stage of screening, 2,880 SNPs were selected by criteria in which several factors such as odds ratios, *P* values of Fisher's exact test, allele frequency and linkage disequilibrium were taken into consideration (see Methods). The 2,880 SNPs were genotyped on separate stage 2 samples (749 cases and 750 healthy volunteer controls), and valid genotype data were obtained for 2,753 SNPs. **Table 1** lists ten SNPs showing the least *P* values for allelic contingency tables in the second stage. Of the ten SNPs, four are located at 8q24.3, where *PSCA* and *LY6K* map (**Table 1** and **Fig. 1a**).

Linkage disequilibrium (LD) analysis of the first-screening data showed that the *PSCA* and *LY6K* genes are in the same LD block. However, our separate dataset on 109,365 SNPs genotyped by Illumina Human-1 BeadChip on 379 Japanese controls offered denser SNP

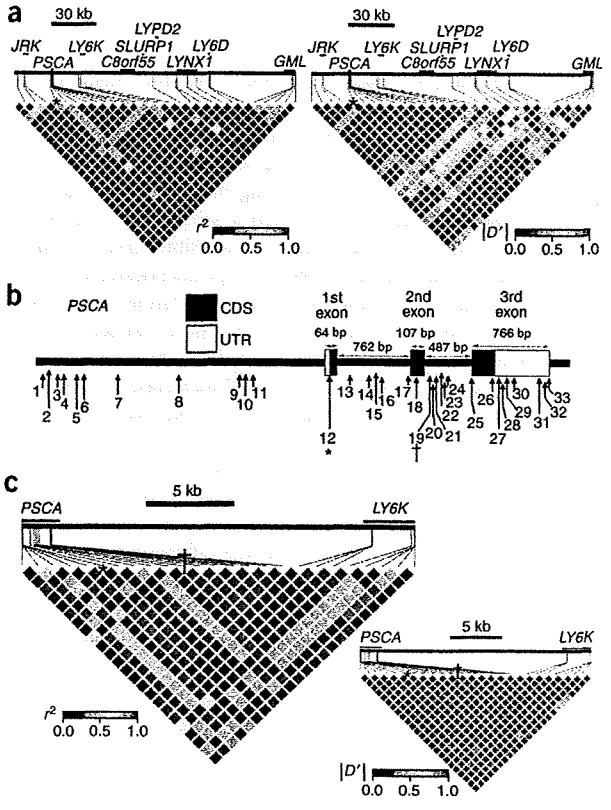

Figure 1 LD analyses of the SNPs in the genomic region around *PSCA*. (**a**) LD maps are shown by two parameters, r^2 and *D'* for 379 Japanese control individuals. The asterisk (*) marks SNP rs2294008. The other SNP, rs2976392, was not on the Illumina Human-1 BeadChip used for drawing the LD map. (**b**) SNPs (arrows) of *PSCA* identified by resequencing. The numbers correspond to those shown in **Table 2**. rs2294008 can modulate the transcriptional activity of the *PSCA* promoter *in vitro*. rs2976392 (†) was identified first by the second screening of this genome scan and is in strong LD with rs2294008. CDS, coding sequence. (**c**) Fine LD maps constructed by typing 750 Japanese control individuals for the 17 common SNPs (numbers 1, 4, 6, 10, 11, 12, 15–19, 22, 26, 27, 29, 30 and 32 in **Table 2**).

© 2008 Nature Publishing Group http://www.nature.com/naturegenetics

Table 2 SNPs in *PSCA* identified by resequencing and their association with diffuse-type gastric cancer in the stage 2 case and control subjects

				Resequencing		Genotyping on 749 cases and 750 controls				
SNP No.	Nucleotide position	rs number	SNP function	A/a	MAF	OR	95% CI	*P* (Fisher)	Risk allele	MAF
1	143755946	–	–	C/T	0.11	1.14	0.92–1.42	0.22	–	0.14
2	143756023	–	–	C/T	0.01	–	–	–	–	–
3	143756101	–	–	G/T	0.01	–	–	–	–	–
4	143756139	rs2978981	5′ flnk	T/C	0.29	1.59	1.36–1.86	4.0×10^{-9}	T	0.38
5	143756303	–	–	G/T	0.02	–	–	–	–	–
6	143756366	rs2976387	5′ flnk	A/G	0.42	1.61	1.39–1.86	1.2×10^{-10}	A	0.48
7	143756700	–	–	C/T	0.02	–	–	–	–	–
8	143757423	rs2976389[a]	5′ flnk	C/T	0.22	–	–	–	–	–
9	143758036	–	–	A/C	0.01	–	–	–	–	–
10	143758105	rs6471587	5′ flnk	C/G	0.35	1.14	0.92–1.41	0.24	–	0.14
11	143758174	rs13262164	5′ flnk	C/T	0.16	0.73	0.62–0.86	1.5×10^{-4}	T	0.26
12	143758933	rs2294008	Met/(Thr)[b]	T/C	0.33	1.58	1.35–1.85	6.3×10^{-9}	T	0.38
13	143759137	rs2920279[c]	Int	C/A	0.34	–	–	–	–	–
14	143759334	–	–	C/G	0.01	–	–	–	–	–
15	143759392	rs2294009	Int	G/A	0.01	1.02	0.61–1.73	1.0	–	0.03
16	143759432	rs2294010	Int	G/A	0.37	1.58	1.35–1.85	5.1×10^{-9}	G	0.38
17	143759726	rs2976391	Int	C/A	0.43	1.42	1.17–1.72	3.2×10^{-4}	C	0.20
18	143759809	rs3736001	Glu/Lys	G/A	0.09	1.22	0.95–1.56	0.11	–	0.11
19	143759934	rs2976392	Int	A/G	0.33	1.62	1.38–1.89	1.1×10^{-9}	A	0.38
20	143759969	rs3736003	Int	C/T	0.10	–	–	–	–	–
21	143759996	–	–	C/G	0.01	–	–	–	–	–
22	143760045	rs2920298	Int	G/A	0.21	1.58	1.35–1.85	5.0×10^{-9}	G	0.38
23	143760085	rs2920297[c]	Int	G/A	0.32	–	–	–	–	–
24	143760111	rs2920296[c]	Int	G/A	0.34	–	–	–	–	–
25	143760322	–	–	G/A	0.01	–	–	–	–	–
26	143760549	rs1045531	Leu/Leu	A/C	0.30	1.58	1.35–1.85	4.8×10^{-9}	A	0.38
27	143760624	rs2976394	3′ UTR	T/C	0.33	1.59	1.36–1.86	3.5×10^{-9}	T	0.38
28	143760654	–	–	A/T	0.03	–	–	–	–	–
29	143760692	rs10216533	3′ UTR	A/G	0.33	1.59	1.36–1.86	3.6×10^{-9}	A	0.38
30	143760752	rs2976395	3′UTR	A/G	0.25	1.59	1.36–1.86	3.9×10^{-9}	A	0.38
31	143760960	rs1045574[a]	Int	A/G	0.32	–	–	–	–	–
32	143761003	rs2976396	3′ UTR	A/G	0.34	1.59	1.35–1.86	4.9×10^{-9}	A	0.38
33	143761011	–	–	C/A	0.01	–	–	–	–	–

Position based on NCBI Build 36. SNP information obtained from dbSNP database. 5′ flnk and 3′ UTR for those SNPs located in the 5′ flanking region and 3′ untranslated region of the *PSCA* gene, respectively, and Int for intronic SNPs. SNPs in the coding region are shown for their effects on amino acid sequence (major allele/minor allele). Major/minor alleles and minor allele frequency were obtained by resequencing of 48 Japanese individuals. Risk allele and control minor allele frequency were obtained by an association study on the stage 2 subjects (749 cases and 750 controls). Dash in an empty cell means that the information is either unavailable or irrelevant.
[a]SNP not genotyped because TaqMan Assay-by-Design development was not successful. [b]When this codon codes for methionine (T allele), it is considered the translation starting site. For C allele, the protein may be translated from the next downstream methionine (**Supplementary Fig. 10** online). [c]SNP not genotyped because of their intronic location and closeness to other SNPs to be typed.

typing data and showed separation of the two genes into different blocks. Moreover, the association of the *LY6K* SNP with diffuse-type gastric cancer was neither significant after Bonferroni correction nor supported by permutation test (**Table 1**). Because no other known gene exists in the LD blocks (**Fig. 1a**), we assumed that the *PSCA* polymorphisms are responsible for the observed association with diffuse-type gastric cancer, and that the relatively low *P* values of the *LY6K* SNPs, albeit not significant after Bonferroni correction, are due to the LD between *LY6K* and *PSCA*.

We then resequenced *PSCA* and its 5′ upstream region on 48 Japanese controls and identified 33 SNPs (**Fig. 1b** and **Table 2**). After excluding some of the rare SNPs (minor allele frequency (MAF) <0.11) and several SNPs incompatible with our typing platform, we genotyped 17 SNPs on 749 cases and 750 controls (**Table 2**). Saturation genotyping on the *PSCA* SNPs revealed the presence of several other statistically significant SNPs, including a missense SNP located at the presumed translation-initiating codon, rs2294008 (OR = 1.58, 95% CI = 1.35–1.85, $P = 6.3 \times 10^{-9}$; **Table 2**).

Next, we inferred the haplotype structure of *PSCA* using the SNPs identified in the resequencing. We focused on both the 5′ upstream and the exonic regions of the gene and found four haplotypes in the upstream region determined by five SNPs, and three haplotypes in the exons determined by seven SNPs (**Table 3**). Odds ratios of each haplotype against the other haplotypes were calculated on the genotyping data (**Table 2**) on the 749 cases with diffuse-type gastric cancer and 750 controls. The odds ratio and its *P* value were not substantially improved by the haplotype analysis as compared to the single SNP–based analysis. Moreover, both upstream and exonic haplotypes contain rs2294008, the only statistically significant missense SNP, and the odds ratio and *P* value of the haplotype seem to depend simply on the fraction of the rs2294008 risk allele, T, in the case and control subjects (**Table 3**). Together with a reporter assay described

© 2008 Nature Publishing Group http://www.nature.com/naturegenetics

Table 3 Haplotypes for functional analyses in the exonic and upstream regions of *PSCA* and their association with diffuse-type gastric cancer

	Frequency					
Haplotype ID	Case	Control	OR	95% CI	*P* (Wald)	SNP No. list in the haplotype
Exonic region						12-18-26-27-29-30-32
PSCA-ExH1	0.63	0.51	1.6	1.4–1.9	5.9×10^{-11}	T- G- A- T- A- A- A
PSCA-ExH2	0.09	0.11	0.82	0.65–1.0	0.11	T- A- A- T- A- A- A
PSCA-ExH3	0.28	0.38	0.63	0.54–0.74	5.0×10^{-9}	C- G- C- C- G- G- G
Upstream region						4- 6-10-11-12
PSCA-UpH1	0.32	0.26	1.4	1.2–1.6	1.6×10^{-4}	T- A- C- T- T
PSCA-UpH2	0.28	0.22	1.3	1.1–1.6	6.1×10^{-4}	T- A- C- C- T
PSCA-UpH3	0.13	0.14	0.88	0.71–1.1	0.23	T- G- G- C- T
PSCA-UpH4	0.28	0.38	0.63	0.54–0.74	4.9×10^{-9}	C- G- C- C- C

Haplotype frequencies in the 749 cases and 750 controls analyzed for the stage 2 screening of the genome scan. Odds ratio and 95% CI were calculated from a contingency table based on the estimated haplotype frequencies. *P* values were calculated by Wald statistics assuming a multiplicative model. SNP number is defined in **Table 2** and **Figure 1b**; in the upstream region, SNPs 4–11 are at –2.8, –2.5, –0.8 and –0.76 kb upstream of the transcription starting site, respectively.

© 2008 Nature Publishing Group http://www.nature.com/naturegenetics

later, the resequencing-based high-density genotyping analysis suggests that rs2294008 is most likely responsible for the association, although other possibilities could not be excluded completely, such as polymorphisms undetectable by resequencing, accumulation of rare variants on a certain haplotype or simply other intronic or synonymous SNPs in this region with strong LD (**Fig. 1c**).

PSCA SNP effect larger in diffuse than in intestinal type

We examined the association of the SNPs in *PSCA* with intestinal-type adenocarcinoma by typing 11 SNPs on 599 cases and 648 controls. **Table 4** summarizes the results on two representative SNPs, which showed significant associations with diffuse- but not intestinal-type adenocarcinoma. When all the subjects genotyped on these SNPs in this study are combined (that is, those from the first and second screening, additional fine mapping and control typing for intestinal-type gastric cancer), our case-control panel consists of 932 diffuse-type gastric cancer cases and 1,398 controls for association analysis. Comparison of the dominant and recessive models suggested that the former fits better statistically to explain the effect of the SNPs, although detailed molecular mechanistic discussion should await further biological analyses. The confidence intervals for the odds ratio of the rs2976392 SNP for the intestinal and diffuse types did not overlap in the dominant model. Moreover, the allele and genotype frequencies of the rs2976392 SNP were significantly different between the two types of cancers ($P = 6.0 \times 10^{-4}$), suggesting that the effect of the *PSCA* polymorphisms is different between the two and is not significant in the intestinal type.

PSCA expressed in differentiating gastric epithelial cells

PSCA was originally identified as a prostate-specific stem cell antigen[20,21], and its expression was also reported in the bladder, esophagus and stomach[22]. However, the precise region of its expression in the gastric epithelium has been unknown. On the surface of the gastric mucosa, epithelial cells form tubular units that consist of four regions from the surface to the bottom: the pit, isthmus, neck and base regions

Table 4 Association of the SNPs in *PSCA* with two major gastric cancer types in Japan

	Case genotype			Allele model			Dominant model			Recessive model		
Type	AA	Aa	aa	OR	95% CI	*P* (Fisher)	OR	95% CI	*P* (logistic)	OR	95% CI	*P* (logistic)
rs2976392 (SNP No.19): risk allele (A) frequency in 1,397 control subjects = 0.616												
Diffuse 926 cases	469	419	38	1.71	1.50–1.94	1.5×10^{-16}	4.24	2.92–6.29	6.4×10^{-18}	1.66	1.39–1.99	1.5×10^{-8}
Intestinal 599 cases	268	272	59	1.29	1.12–1.49	5.0×10^{-4}	1.55	1.13–2.16	0.0059	1.24	1.02–1.52	0.035
1,397 controls	536	650	211	–	–	–	–	–	–	–	–	–
Intestinal vs. diffuse	–	–	–	1.32	1.13–1.56	6.0×10^{-4}	2.73	1.67–4.56	3.3×10^{-5}	1.35	1.07–1.71	0.012
rs2294008 (SNP No. 12): risk allele (T) frequency in 1,396 control subjects = 0.617												
Diffuse 925 cases	461	426	38	1.67	1.47–1.90	2.2×10^{-15}	4.18	2.88–6.21	1.5×10^{-17}	1.62	1.35–1.93	9.4×10^{-8}
Intestinal 599 cases	267	274	58	1.29	1.11–1.49	5.1×10^{-4}	1.59	1.15–2.21	0.0041	1.24	1.01–1.52	0.040
1,396 controls	536	650	210	–	–	–	–	–	–	–	–	–
Intestinal vs. diffuse	–	–	–	1.30	1.10–1.52	0.0015	2.70	1.64–4.50	4.7×10^{-5}	1.35	1.06–1.71	0.013

Genotypes are shown as AA for risk allele homozygotes, Aa for heterozygotes and aa for the nonrisk allele homozygotes. For dominant and recessive models, gender- and age-adjusted OR, its 95% CI and *P* values calculated by exact logistic regression are shown. Allele and genotype frequency differences between the intestinal- and diffuse-type gastric cancers were tested for statistical significance.

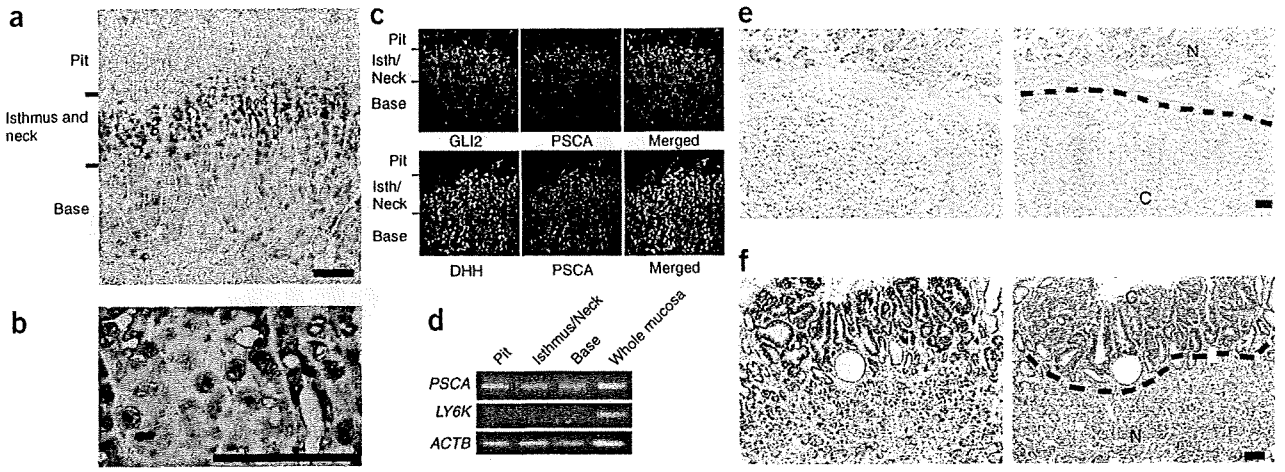

Figure 2 Expression of *PSCA* in the gastric epithelium. **(a)** Immunohistochemical double staining showed the presence of PSCA (blue staining) and PCNA (brown nuclear staining). Although PSCA protein was detected mainly in the cells of the isthmus and neck region, it was also expressed in some cells in the base region. Scale bar, 100 μm. **(b)** A higher magnification of **a**, showing colocalization of the PSCA protein (blue) with some, but not all, of the PCNA-positive cells (brown nuclear staining). Scale bar, 100 μm. **(c)** Immunohistochemical double staining of human gastric epithelium for GLI2 and PSCA and for DHH and PSCA. GLI2, a pit-cell lineage marker, and DHH, a parietal-cell lineage marker, are expressed mainly in the pit and base regions, respectively, although both were also observed in the isthmus/neck region. Merged figures show colocalization of PSCA with GLI2 and DHH. **(d)** RT-PCR analysis on the laser-captured microdissection samples showing *PSCA* transcripts in the pit, isthmus/neck and base regions. *LY6K*, which is located next to *PSCA* on human chromosome 8q24.2 (**Fig. 1**), was not expressed in the gastric epithelial cells. **(e,f)** Double staining for PSCA (blue) and PCNA (brown) proteins (left panels) showed silencing of PSCA in the diffuse-type **(e)** and intestinal-type **(f)** gastric cancer cells. Right panels show hematoxylin-eosin staining of the adjacent sections, indicating noncancerous (N) and cancerous (C) portions. Blue staining of the normal gastric glands is scored as 'positive' **(e,f)**, whereas those of the diffuse- and intestinal-type gastric cancers are 'negative' **(e)** and 'weakly positive' **(f)**, respectively. Scale bar, 100 μm.

© 2008 Nature Publishing Group http://www.nature.com/naturegenetics

(**Fig. 2a**). The isthmus is considered to contain stem cells and precursors of three cell lineages that move and differentiate to mature mucus-secreting pit cells (pit-cell lineage), hydrochloric acid–producing parietal cells (parietal-cell lineage) and mucus-secreting neck cells and pepsinogen-producing zymogenic cells (zymogenic-cell lineage)[24,25]. Diffuse-type gastric cancer may originate from the stem cells and/or the three precursors in the isthmus[7].

We raised a monoclonal antibody to PSCA and confirmed its specificity by flow cytometry and immunohistochemical analyses (**Supplementary Figs. 2** and **3** online). The PSCA protein was detected mainly in the middle portion of the gastric epithelium or isthmus and overlapped with the region where a proliferating-cell marker, proliferating cell nuclear antigen (PCNA), was also expressed (**Fig. 2a**). In the isthmus, PSCA protein was detected in cells with a variety of shapes, sizes and amounts of PCNA (**Fig. 2b**), suggesting that it is expressed both in precursor cells, such as pre-pit and pre-neck cells, and in differentiated cells, such as parietal cells. Double staining showed that PSCA and a pit-cell lineage marker, GLI2 (ref. 26), were coexpressed in some cells in the isthmus and neck regions. Similarly, PSCA and a parietal-cell lineage marker, DHH[26], were found to be colocalized in some cells in the region (**Fig. 2c**). The coexpression with the lineage markers in the isthmus region suggests that PSCA is expressed both in the pit- and parietal-cell lineages. In addition, several cells with weak staining were also observed in the pit and base regions (**Fig. 2a** and **Supplementary Fig. 4** online). We carried out RT-PCR analysis on the microdissected human gastric epithelium and detected *PSCA* transcripts in the pit, isthmus, neck and base regions (**Fig. 2d**). In sum, the results of the expression studies suggested that the PSCA protein is mainly expressed in the isthmus, probably in a variety of cell lineages and differentiation stages, with various proliferation activities. PSCA protein was undetectable in the normal intestinal epithelium and was downregulated in the gastric tissue with intestinal metaplasia (**Supplementary Figs. 3** and **4**).

Among cancerous tissues, quantitative RT-PCR (**Supplementary Fig. 5** online) and immunohistochemical (**Fig. 2e,f** and **Supplementary Fig. 6** online) analyses showed frequent suppression of PSCA expression in both the intestinal and diffuse types. However, when the immunohistochemical staining was scored in three grades—positive, weakly positive and negative—all 19 diffuse gastric cancer tissues analyzed were negative, whereas 20 out of 21 intestinal cancer tissues showed weakly positive staining, with the remaining one being negative. In all, the PSCA downregulation seemed more pronounced in the diffuse type by immunohistochemistry.

Cell-proliferation inhibition activity of *PSCA*

It has been suggested that PSCA is involved in the cell-proliferation inhibition of prostate epithelial cell lines[27,28]. Among the 12 gastric cancer cell lines we examined, HSC57 and some others did not express *PSCA* (**Supplementary Fig. 5**). We stably transfected *PSCA* cDNA to HSC57 and found that cells with *PSCA* showed fewer G418-resistant colonies than those without *PSCA*, indicating that PSCA has a cell-proliferation inhibition and/or cell-death induction activity (**Fig. 3a**). We isolated four clones with different amounts of *PSCA* expression (**Supplementary Fig. 7** online) and found that those with *PSCA* expression, HSC57P1, HSC57P2 and HSC57P3, showed a slower growth rate than HSC57P0, which did not have *PSCA* expression (**Fig. 3b**). We examined whether the growth suppression of the *PSCA*-transfected cells was due to a significant difference in the number of dead cells. The results suggested that *PSCA* does not induce significant cell death (**Supplementary Fig. 8** online and data not shown).